

ANALYSIS OF DIPMETER LOGS

PART 1 - EVOLUTION OF DIPMETER TOOLS

BY

E.R.CRAIN, P.ENG.

**Spectrum 2000 Mindware Ltd
Calgary AB**

Abstract

This two part series is an extract from the "Dipmeter Theory and Data Processing" chapter of The Log Analysis Handbook - Volume 2, soon to be published by Pennwell Books. It covers everything you ever wanted to know about dipmeter tools and computer displays, but were afraid to ask your supplier. Part 1 covers The evolution of tools and processing techniques.

Part 2, to be published in the next CWLS Journal, will cover dipmeter presentations, and the arithmetic of dip manipulations. For my treatment of how to analyse dipmeter patterns, you'll have to wait for the book.

I have attempted to provide an impartial review, but trade names and suppliers names are mentioned where appropriate. If any service company feels short changed by my treatment of their tools and techniques, I would appreciate receiving updated information from them.

If you have as poor a memory as I have, you may find this review useful when analysing dipmeters. I don't think anyone, except a service company salesman, could remember all the variations which have been produced over the years.

Introduction To This Chapter

Because the dipmeter is such an important tool for geological analysis of structure and stratigraphy, it deserves its own Chapter, as a prerequisite to the next chapters. Both tool design and computation methods play a role in the type, quality, and quantity of geological data that can be derived from dipmeters.

One of the major sources of information for developing exploration plays is, of course, data in existing well files. Logging tool design and data presentation have evolved dramatically over the sixty year history of logging. As a result, the log analyst will be faced with a wide variety of data quality, depending on the age of the well file. For this reason, we review the evolution of dipmeter tools, dipmeter calculation methods, and dipmeter presentation methods in considerable detail. From this, you should be able to decide if the available data will answer any of the geological questions you may wish to pose.

The Chapter is organized around three main topics:

1. tool types
2. computation methods
3. data presentation methods

If you plan to use existing dipmeter data for serious exploration, you must be aware of the differences and limitations of each tool and computation method.

While the primary source of structural information from logs is the dipmeter, corroborative evidence from correlation to offset wells, oriented core data, and seismic data is needed to confirm or deny some analyses. There is often more than one plausible solution to the analysis of structural and stratigraphic problems.

Evolution of the Dipmeter Concept

In the beginning, there were no dipmeters. Dip magnitude and direction of rock strata was assessed by knowing the subsea elevation of a distinctive rock layer in three or more wells which were closely spaced. The equation of a plane is defined by the X, Y, and Z coordinates of three points, so the elevations and well locations were sufficient data to define dip. Subsurface mapping of clearly defined formation markers is widely used today to estimate both regional and local dips. Measurement of dip in outcrop is also widely used to assist in mapping overall basin structure. Neither of these methods will find structures located between the control points because there is insufficient data.

In 1933, attempts were made to evaluate dip by analyzing resistivity anisotropy effects on a modified electrical log. The resistivity of a layer is usually lower parallel to the bed than perpendicular to it. By taking resistivity

measurements with suitably arranged electrodes, the dip direction of thick, well stratified beds could be found. The dip angle had to be known from cores, and the hole direction had to be measured. This was possible using a device called an electromagnetic teleclinometer, which sent a signal up the logging cable proportional to the tool's deviation from the vertical. From this data, a crude dipmeter survey was presented. It is doubtful that any copies survive in well files. More modern data is often available in any event.

The anisotropy dipmeter was supplanted in 1943 by a tool using three simultaneous spontaneous potential measurements oriented 120 degrees apart around the circumference of the logging tool. Using the same principle that three points define a plane, the tool provided sufficient data, along with bit size, deviation, and direction, and tool orientation in the hole, to calculate dip. The three points were taken as the bed boundaries defined by the SP curve from each electrode.

The balance of the data came from a photoclinometer survey taken at stations near the top and bottom of the recorded intervals of the dipmeter curves. A schematic example of the concept is shown in Figure 5.01. The photoclinometer consisted of a magnetic compass, a ball bearing in a graduated curved dish, and a camera that photographed these components on demand.

This sounds simple. However, the magnitude of dip which is of interest in exploration is from a fraction of 1 degree to vertical. This poses serious constraints on tool design and data analysis. For example, a regional dip of about 50 ft/mile is equivalent to 1/2 degree dip. Local structure or drape over deeper erosional surfaces may modify this dip to flat or 1/2 degree in another direction. In some areas this is significant and could define the trapping mechanism. The dipmeter device, the recording process, and the curve correlation methods must have sufficient resolution to enable us to see this small difference.

A bed dipping at 1/2 degree across a 9" borehole will be less than 1/10 inch higher on one side of the hole than on the other. The displacement between curves shown on Figure 5.01 will be less than 0.1 inches if recorded at 12 inches per foot of borehole. If recorded at 5 inches per hundred feet, a normal detail logging scale, this displacement would be only 0.0004 inches on the film. As a result, scales of 60 inches per 100 feet were used. Now the 1/10 inch displacement is represented by 0.005 inches - a measurable distance on the film.

Due to the relatively round shape of the SP curve at most bed boundaries, this level of resolution was not achieved with the SP dipmeter. Moreover, the tool was useless in carbonates where SP does not develop well. The only dips presented were those from major bed boundaries where dip was steep enough to be obvious.

Although the SP dipmeter was abandoned quickly in favour of three resistivity curves, the photoclinometer survived well into the 1960's as a directional survey tool. A sample is shown in Figure 5.02. In addition to the photographs of the compass and deviation ball, typed listings of computed results and a plan of the well track were presented (Figures 5.03 and 5.04). Since the well bore often deviated, without any help from the drilling crew, to keep the bit perpendicular to the formation dip, the directional survey data was sometimes

used as a guide to dip.

The resistivity dipmeter used three lateral curves instead of SP curves, mounted on the same rubber arms as were used for the SP version. Accuracy was better in hard rock areas. A sample is shown in Figure 5.05. Both SP and resistivity dipmeters were only recorded over selected intervals, chosen by observation of the other open hole logs. Only short intervals where there is lots of curve action were suitable for dip computation.

Typical computed results from the SP or resistivity dipmeter are shown in Figures 5.06 and 5.07. Although rare, examples can be found in files for wells drilled in the 1940's.

In 1950, better accuracy was obtained by a newly designed dipmeter utilizing three microlog resistivity pads. Now a continuous log could be made, and with very detailed resolution from the microlog pads, a fine scale dipmeter was a reality. In 1952, the microlog pads were replaced with microlaterlog 3 pads which measured conductivity instead of resistivity.

Orientation data was recorded simultaneously and continuously with a device called a poteclinometer. Data consisted of hole deviation angle, relative bearing (which describes the angle to the high side of the hole from pad number one), and the azimuth (which describes the angle between north and pad number one). This is sufficient data to orient the dip azimuth and the direction of hole deviation. The algebra is described later in this Chapter.

This eliminated the need to stop the tool to take pictures with the photoclinometer. Directional surveys run with this equipment were also more accurate, but considerably more expensive. The optical comparator was also developed during this period (see next section for details of its use). This increased dip accuracy further by reducing errors in measuring the offset between traces.

The computed data was presented in the same tabular and graphical fashion as previously (Figures 5.06 and 5.07), but with considerably higher frequency. However, by 1958, some hardy souls were plotting individual dips as small arrows on a graph of dip magnitude versus depth. The direction of the arrow represented the dip direction relative to a compass rose with north at the top, as in Figure 5.08. This was the precursor to the now common arrow plot, sometimes called a tadpole plot, generated by computer. Computer plotting was first seen around 1961.

The first attempts to legitimately use detailed dip data for stratigraphic evaluation occurred around 1955. An example of the difference in data quality and quantity between short interval and continuous data is shown in Figure 5.09. The raw data was recorded at 60 inches of log for 100 feet of wellbore, or 1:20 scale, shown half size in Figure 5.10. Literally miles of this photographic paper was developed, processed, and sifted through the optical comparator each month. Most of it has deteriorated or been destroyed and is not available for recomputation.

Fortunately, beginning in 1961, dipmeters were recorded on digital magnetic tape, reducing and finally eliminating the need for the detailed paper logs. The offsets between traces were derived by computer correlations, leading to a

whole new language: correlation window, step length, search angle, etc.

Modern Dipmeters

In 1969, a new four pad high resolution dipmeter was introduced. The electrode had even finer resolution than the microlaterolog pads and the electronics were improved to transmit data at a higher rate, so that the well could be logged faster and finer bedding features could be recorded. Four pads allowed for calculation of four different sets of 3-point planes as well as a four point curved surface or a "best fit" flat surface. Program logic could compare all results and eliminate bad correlations, or grade the results to show how well the different results matched.

A special "speed button" on one pad provided information to the program to compensate for minor speed differences as the tool moved up the hole. These variations created scatter in the computed results (Figure 5.11). In addition, a synthetic resistivity curve was generated from the dip curves, to be used as a correlation curve.

The geometry of a four pad device is shown schematically in Figure 5.12 and the arrangement of tool components in Figure 5.13. Typical raw data curves and an answer plot are found in Figure 5.14.

In 1975, secondary computer processing, called CLUSTER (Schlumberger trademark) or SHIVA (Gearhart trademark), were developed to validate the results from the standard program. Other secondary programs were developed to enhance stratigraphic features, notably GEODIP (Schlumberger trademark). These processes are described later.

About 1980, three axis accelerometers and three axis magnetometers replaced the magnetic compass, relative bearing, and hole azimuth potentiometers. However, the log still presented these three curves, derived now from the solid state sensors instead of the more failure prone electromechanical devices.

A further refinement in 1983 created the stratigraphic high resolution dipmeter. An additional electrode set was added to each pad giving eight dip correlation curves instead of four. With this number of measurements, the results can be presented more often, as many as 10 or 20 per foot if desired, instead of the more usual 1 or 2. Better speed correction is provided by accelerometer data from sensors inside the tool. Typical raw data plot is shown in Figure 5.15. A six arm dipmeter has also been developed to meet the need for stratigraphic information, with a lower cost tool.

Three dip computation modes are available from the stratigraphic high resolution dipmeter. First is the usual pad to pad correlation, which benefits from the extra redundancy of two electrodes per pad. This is called Mean Squares Dip or MSD, and often is used for structural or regional dip analysis. The dip is a weighted average of all pad to pad dips. In strongly parallel beds, the result is very good, but in cross bedded formations with varying dip, the average dip has little significance, except to show overall direction of dip.

Second is called Continuous Side by Side or CSB dip correlation using only the individual electrode pairs on each pad. Dip vectors from adjacent electrode pairs are used to define dip. CSB dips respond to short interval, low contrast changes often characteristic of internal layering in clastics, but also will respond to high contrast structural dips. It is very useful for structural dip analysis in high angle apparent dip, greater than 50 degrees. In finely bedded rocks exhibiting cross bedding, considerable detail can be shown if the correlation length and step distance are kept fairly short.

Third are pad to pad correlations using a pattern recognition rather than cross-correlation system. This is called Local Dip or LOC dip and responds to nonrepetitive events such as erosional surfaces or breaks in the depositional sequence. A comparison of the three modes with normal high resolution dipmeter results is shown in Figure 5.16. It is now possible to analyze data with a resolution of a few inches and compare it to core data (Figure 5.17).

In 1986, the "ultimate" dipmeter was developed, called the formation microscanner. Using an additional 27 electrodes on each of two pads of the dipmeter, each pad records 27 microresistivity curves spaced 1/10 inch apart on the borehole surface. Each pad covers a 2.8 inch wide portion of the circumference of the well bore. Several passes over the interval will often provide virtually complete coverage of the rock face.

A microscanner tool with fewer (sixteen) electrodes per pad, but with four imaging pads, is now available, and provides better coverage of the well bore wall than the two pad version. An eight pad version is being released as this Chapter goes to press. The electrodes are smaller, allowing for higher resolution, but are spaced to provide the same wall face coverage, about 2.5 inches per pad. In an 8 inch diameter hole, electrode coverage is about 80% and in a 6 inch hole is greater than 100%. This overcomes one of the major complaints about the FMS, namely the number of passes needed to obtain a complete image of the well bore.

The resistivity traces are translated into images based on their relative resistivity values, in either black and white or colour. The gray scale or colour spectrum can be stretched or squeezed in the computer to enhance certain features, such as porosity, fractures, or shale laminations. Images can be plotted at the same scale as the core photographs for comparison. A sample is given in Figure 5.18.

The primary use of the tool is for identification of irregular features, such as vugs and fractures, for accurate sand counts in thin bedded zones, and for identifying stratigraphic features. If sufficient rock face is imaged, dips can be found by digitizing the bedding planes visible on the microscanner image, or by automatic computation using all valid image traces. Note that a planar, dipping, bedding plane will trace a sine wave on a circumferential image, such as those made by the microscanner or a borehole televiewer.

The dips found by FMS dip processing are superior to CSB or LOC dips because a larger number of resistivity traces can be used in the calculation. They can be computed automatically and displayed on the FMS image. In addition, calculated dips can be edited or removed, and new bed boundary correlations picked with a mouse on an interactive CRT image. Thus dips that pass or fail preconceived

processing criteria can be deleted or added as the analyst desires. An example of this technique is shown as a case history in Chapter Seven.

A microscanner has about 10 times the spatial resolution of a televiewer and 500 times the amplitude resolution, due to the difference in contrast between the resistivity and acoustic impedance ranges measured by the respective tools.

A dipmeter for use in nonconductive mud systems was introduced in 1988. It uses microinduction resistivity measurements instead of the usual electrical resistivity pads. A knife blade electrode version was used before this invention.

Basic Continuous Dipmeter Calculations

The computation of dipmeter data has been handled in one of three general ways: manual processing, combination of manual and computer processing, and total computer processing.

Manual correlation and computation methods were developed first and there are several different methods of doing the work. The dipmeter curves must first be correlated; this may be done by slipping a print of a log under the film used to make the print and measuring the depth displacement between peaks and valleys on the curves. Pad number one is used as a reference to measure displacements to each of the other curves.

Another method of curve correlation uses an optical comparator, a system of mirrors and lenses which allow the user to optically lay one curve over another and shift it up and down. The amount of shift is measured mechanically on a dial and is recorded as the displacement.

After these correlations have been made, the azimuth of the number one electrode, the borehole deviation angle, the relative bearing, and the borehole diameter from the calipers are recorded. This information, plus the depth, is necessary to compute the dip angle and dip direction of a point referenced to magnetic north. Because true dip is referenced to true north, we must also account for magnetic declination of the region.

Mathematical formulas to solve this geometric puzzle are given later in this Chapter. The manual calculation of dip magnitude and direction with the above information was made in several ways: by using a calculator and trigonometric tables, a scientific programmable calculator (after 1970) with trig functions, a mathematically derived physical computing device (in other words, an analog computer), or stereographic nets, the latter being the most common manual method used in the past. A very small amount of hand calculator work is still done today.

Another method of dipmeter computation utilized manual correlation and computer reduction of the data. This type of processing was originally developed to minimize turnaround time and to allow the tedious, time consuming computation and plotting of results to be performed by a digital computer. This may still be done today for recomputation of continuous dipmeters recorded on paper, or

on 7 track digital tapes (which are unreadable by most modern computers) for which the paper records are still available.

The most recently developed system of computation is computer correlation and calculation from data on digital magnetic tape. The data from the magnetic tape is entered into a digital computer and processed. In the correlation program, the digital information representing the dipmeter curves is stored in memory and the data from one trace is compared to the other traces to determine the vertical displacement between the traces. After these displacements are calculated, the tool orientation information is used to compute the actual formation dips.

The standard correlation process is performed by a mathematical function called cross-correlation, in which the offset distance between events on two curves are found. The distance between the center and the maximum amplitude on the correlogram indicates the displacement between the two curves. The offsets for all curve pairs are then adjusted to obtain the offsets relative to the center of the correlation interval. More exotic forms of correlation, some based on pattern recognition theory, are used in the newer programs.

The length of the portion of the curve being correlated is called the correlation interval, correlation length, or correlation window. Correlation interval is usually between one and four feet, but can be smaller or larger. The correlation is calculated at regular intervals along the log. The distance between correlations is called the step distance and is usually 1/2 to 1/4 of the correlation interval. One dip value is calculated at the center of each correlation window, and the dip value is plotted at each step distance.

In order to determine how far up and down each adjacent curve the correlation is to be performed, a search angle is defined. In moderate structural dip the search angle is usually 45 degrees, but if expected dips are low, the angle can be reduced to eliminate noise, or spurious dips caused by erratic wiggles on the curves. Some computer programs use a search length instead of a search angle. In steep dips, a higher search angle is required. These terms are illustrated in the top half of Figure 5.19.

The number of dips computed from computer processed logs can be any density required for a particular purpose. For structural analysis, normal densities range from one computation every one or two feet to one computation every ten feet. In those instances where additional information is required, such as for stratigraphic analysis, points as close as every few inches can be computed.

The usual way to describe these parameters is in the form CORR x STEP x ANGLE. For example a 4 x 1 x 45 process uses a 4 foot correlation, a 1 foot step, with a 45 degree search angle. The recommended defaults for dipmeter processing are:

Low angle structural dip: 4 x 2 x 45
eg: normal or reverse faults, folds

High angle structural dip: 8 x 4 x 80
eg: overthrust faults, recumbent folds

Sand body stratigraphic dip: 2 x 1 x 30
eg: beach, bar, channel, drape

Complex stratigraphic dip: 1 x 0.5 x 30
eg: submarine fan, scree slope, turbidite

A fourth parameter is sometimes used to indicate that the program can search farther up the curve if no correlation is found. This is shown as:

4 x 2 x 35 x 2

which allows the program to use a 70 degree search angle after failing at 35 degrees.

The effect of a shorter correlation interval is shown in the bottom illustration of Figure 5.19, where only regional dip is found in the long interval case, and stratigraphic dip is superimposed on the regional when a short interval is used. The problem with dip determination by cross-correlation is that it does average all dips found in the correlation interval. If both structural and stratigraphic dips are present, the average may not reflect either of them correctly, regardless of the correlation interval. Regional dip is therefore usually chosen in a nearby shale or bedded carbonate thick enough to give an accurate result, without interference from stratigraphic events.

Many dipmeters have been computed with inappropriate parameters and could be improved by recomputation with a better choice of values. The defaults shown above are just starting points. In particular, parameters for steeply deviated holes may need considerable experimentation and variation throughout the hole.

Handling Correlation Closure Error

To compute the displacements between the wiggles on a three curve continuous dipmeter, we could correlate at each computation level, defined by the correlation length, a segment of curve 1 with curve 2 first, and then correlate a segment of curve 2 with curve 3. The two displacements found would be sufficient to determine the dip. However, we might just as well have correlated curves 2 and 3 then curves 3 and 1, or curves 3 and 1 and then 1 and 2. All three combinations of displacement pairs should in theory define the same bedding plane, and the same dip. If they do not, a closure error exists.

In manual correlations, one could correlate three pairs, determining three displacements. For perfect closure, the algebraic sum of the displacements must be zero. Usually, because of the inaccuracy of the optical comparator, a small closure error existed. This error could then be distributed among the three displacements as a small correction before final determination of the dip. In practice, this was an onerous task, and two pairs were often picked with no attempt to determine closure error.

In automatic correlations, two kinds of closure errors can occur: small ones due to minor variations in shape between the three curves, and large errors. Small errors are handled as for manual computation.

When a large error exists, it is because at least one of the correlations is in error - the same geological event is not being picked on all three pairs. In manual correlation, a large error was usually fixed by repicking one of the

correlated curves. For an automatic computation, we have to choose between three possible computable dips, only one of which may be correct. There are no strong mathematical rules to choose the correct dip. If closure error is large, the usual procedure is to compute no result and display no dip arrow.

The three arm tool is also vulnerable to adverse hole conditions. If one curve degenerates, for instance when one pad fails to make a good contact with the borehole wall, the computation of dip cannot be made at all. This happens often in deviated holes or in out-of-round holes, resulting in more intervals with no result.

High Resolution Dipmeter Calculations

Four and six arm tools are less vulnerable to hole problems. These are called high resolution dipmeters. If one curve is unuseable, any three others may still be used to determine dip. Also, the two (or three) independent sets of arms fit elliptical holes better. For these reasons, four and six arm tools have become the preferred dipmeter in recent years.

Six curve pair correlations can be attempted between four curves. The adjacent curve pair displacements are designated respectively as h_{12} , h_{23} , h_{34} , and h_{41} , and the diagonal displacements as h_{13} and h_{24} . These six displacements can in turn be paired in thirteen different ways to provide thirteen dip evaluations for the same level. For the six arm dipmeter, 15 pairs are possible, leading to additional redundancy. The result from each combination is referred to as a dip determination. In recent practice, however, only four or five correlations are made, leading to a maximum of eight possible dip determinations per level. This reduces computer time.

Four arm closure error (E_c) is given by the algebraic sum of the four adjacent curve displacements:

$$E_c = h_{12} + h_{23} + h_{34} + h_{41}$$

For perfect closure, $E_c = 0$.

Three arm closure error can also be computed on a four arm or six arm dipmeter. In this case, closure error is given by the algebraic sum of two adjacent curve displacements and their associated diagonal displacement. This error is distributed around the displacements in proportion to the amount of each displacement.

Handling Correlation Planarity Error

When four or six arm closure exists, or has been created by distributing the error, another error, the planarity error can be measured among the four adjacent curve displacements. Because opposite pairs of pads in the four pad array form a parallelogram, the displacement observed between curves 1 and 2

should be the same as that between curves 4 and 3, and the displacement between curves 2 and 3 should be equal to that between curves 1 and 4. Thus, for perfect planarity:

$$h_{12} = -h_{34} \text{ and } h_{23} = -h_{41}$$

When four arm closure error is zero, planarity error (E_p) is defined as:

$$E_p = h_{12} + h_{34} - h_{23} - h_{41}$$

For perfect planarity, $E_p = 0$. Similar equations exist for the six arm dipmeter.

If closure error is zero and planarity is not zero, then several things may be possible. One is that the bedding may not be planar, such as in the case of festoon current bedding or aeolian dune surfaces. Other possibilities are lack of pad contact with the hole wall and possible miscorrelations. The latter are, in fact, quite likely.

The flow chart in Figure 5.20 shows the complex logic involved in Schlumberger's high resolution dipmeter program. It handles the closure and planarity problems in numerous ways, based on the number and quality of correlations found. The output listing from this program is shown in Figure 5.21. Notice that some of the logic choices are coded on the listing and others on the arrow plot by use of alternate symbols, indicated on the bottom of Figure 5.21.

Dips can also be coded and presented in such a way as to indicate the fact that they are nonplanar. This would help an analyst interpret the bedding, as shown in the example in Figure 5.22, which was processed using Gearhart's OMNIDIP program.

Determining Dip By Clustering and Pooling

The early approach to automatic determination of dip from a four arm dipmeter, described above, was quite arbitrary. The selection procedure was based on:

1. a distribution of closure errors
 2. the elimination of the correlation curve associated with the worst (lowest) correlation coefficient, resulting in a three arm dip determination
- or, if no curve fitted this description, a compromise (average) among the four possible solutions resulting from the planarity error.

None of these approaches used any geological knowledge or any sophisticated statistical aids in the solution.

1. Clustering

The cluster approach for dip selection was developed by Schlumberger to help eliminate the problem of closure and planarity errors. The CLUSTER program name is a registered trademark of Schlumberger. The CLUSTER program does no curve correlation; it operates on output data from an existing dipmeter program. The best reference is Cluster - A Method for Selecting Most Probable Dip Results, V. Hepp and A. Dumestre, SPE Paper 5543, 1975.

The CLUSTER method assumes that correlations are valid if they repeat when the correlation window is moved over a small step distance. If a dominant anomaly exists, it controls the correlation on at least two adjacent dip computations, and it follows that the dominant anomaly defines the same dip value for as long as it is included inside the correlation window.

The scattergram of points shown on Figure 5.23 presents an illustrative plot of all the dips computed from all the retained displacement pairs of ten computation levels. Each dip is plotted at a location on the plot defined by its magnitude and azimuth, and coded to represent a weight indicating the quality of the correlation. There is a great deal of scatter, indicating the noisy nature of the correlated curves. However, two concentrations of points of greater consistency, marked Cluster 1 and Cluster 2, are present.

Redundant dip results thus allow us to choose groups of dips which show some stability throughout the zone and to choose the displacement combinations which contribute dips to the group. Since Cluster 1 represents the greatest concentration of dips, it should be nearest to the dip defined by the dominant anomaly.

If no displacement pair contributes to Cluster 1, then perhaps a contribution is made to Cluster 2 and this, also, should be a valid dip, even though the indication of consistency is not as strong. Failing this, the displacement information must be regarded as meaningless. For such levels no results will be printed on the CLUSTER output listing.

In the example of Figure 5.23, ten levels were grouped together from an arbitrarily selected interval. In the actual clustering procedure an attempt is made to group levels together in a meaningful fashion into short intervals or zones. Zoning is achieved by testing the stability of successive adjacent curve displacements in the input listing.

The test for stability checks the displacement value in the next level upwards to see if it is similar to the current one. If this test is satisfied, over several consecutive levels in at least two contiguous adjacent curve displacement columns, the zone is stable. Zones that do not satisfy these criteria are called open zones. The two types of zones are merely a convenient way to break up the interval for clustering. Both kinds of zones can provide meaningful dips, depending on the quality of the correlations.

Zoning is a preliminary sorting procedure. Both stable and open zones are subsequently treated in the same fashion. Zone length can vary from one to fourteen consecutive displacements. No indication of the zoning used is shown in the output arrow plots or the standard output listing.

The correlation coefficient measured along with the displacement correlation is an important criterion of the quality and is not ignored in the choice of good correlations. To account for this, the dip points placed on the scattergram are weighted according to a coefficient called the level weight. A greater weight raises the contribution of retained dip determinations and enhances their chances of being selected as candidates for clustering.

If the quality of the correlation reported for the level by the source dipmeter program is good, the contribution to the level weight is 3, if fair, it is 2, if poor, it is 1. If the level shows four arm closure (a double asterisk on the original listing), weighting is doubled. Thus, the level weight varies from 1 (poor) to 6 (excellent).

Clusters thus identify the probable ranges of dips for the zone. The program returns to each dip level in turn and retains only those dip determinations which fall within one of the clusters. If one is found in the highest ranked cluster, it is retained, and if there are two or more, their vector average is retained. If none are found, the program can expand the area included in the cluster. If cluster expansion fails, the cluster of next lower rank is checked.

It may happen that no contribution is found from a level to any of the defined clusters, in which case this level is considered to have no result. Similarly, if no clusters are found at all within the zone, no result is shown on the output listing. This occurs when the data are so poor that no meaningful displacement combinations can be made.

Since clustering only uses data from a previously applied dipmeter program, it cannot find new correlations and it cannot find dips where none were found on the original. It may be possible to obtain new results in "no result" intervals by reprocessing the original dipmeter with new parameters.

A typical set of input data to CLUSTER is shown in Figure 5.24 and output for the same interval is shown in Figure 5.25.

The process of dip retrieval that has just been described systematically attempts to provide one dip for each correlation window. However, the basic idea of the method is that consecutive correlation intervals must overlap, in order that dominant anomalies can affect the clustering process. As a result, it is quite usual that the same dip is repeated twice when the overlap between consecutive levels is 50 percent of the correlation length, or four times when the overlap is 75 percent.

Users of dipmeter surveys should train themselves to recognize doublets or quadruplets as representing a single anomaly. However, it would be nice if the computer would do the same and represent it by a single dip result, at the midpoint between the depths of the two or four component levels. This is accomplished by pooling clustered dip results.

2. Pooling

Pooling consists of testing the results from successive levels, up to a number of levels called the pooling constant and controlling whether their angular dispersion does not exceed a fixed value, called the pooling angle. If the test is satisfied, the component dips are replaced by their vector sum, the pooled vector. Its dip magnitude and azimuth are converted to geographic coordinates and printed out at the mean depth, together with other data about the computation. The sample in Figure 5.26 can be compared to the unpooled results in Figure 5.25.

Two separate output files are created: one for the clustered data and one for clustered and pooled data. Thus, in reality, two different dipmeters are created from the same data, using different rules in their analysis.

Figure 5.27 (left side) shows an arrow plot for clustered and pooled results. The arrows with black circles represent high quality ratings. Usually a blackened circle corresponds to pooled results; however, it is possible that a nonpooled result from a high quality level could plot as a blackened circle.

Pooled results are generally plotted on 1 or 2 inch per 100 feet depth scale. This can be done since there are fewer arrows to plot. Thus, one use of pooling is to provide a dip record on a depth scale commonly used for correlation. Usually, structural analysis is all that can be accomplished with this plot.

3. Fan Plots

The arrow plot represents dip magnitude and azimuth from the output listing at their proper depth. However, it does not represent the effect of uncertainties, as represented by the dispersion of dip values and their directions in the original data. The fan plot is a method to present this knowledge as the quality indicator instead of the more usual open or filled circles. A sample is shown on the right side of Figure 5.27.

In the fan plot presentation, a small circle surrounds the center value of dip magnitude. A small line segment extends on both sides from a lower to a higher dip magnitude value, essentially indicating an error bar. In similar fashion, a fan extends from a lower to a higher dip azimuth value. These values are determined from the combination of the pooled dip magnitudes and azimuths and the angular dispersion parameters. They encompass all values within one standard deviation from the mean. The length of the fan represents the number of dips used in the statistic. Thus, it is probable that the true dip is contained inside the possible values within the fan, both in magnitude and azimuth.

The same value of the angular dispersion parameter may correspond to a nearly closed fan at high values of dip to a wide open fan near zero dip magnitude. When angular dispersion exceeds dip magnitude, the azimuth value cannot be specified with any kind of certainty and no fan is drawn.

Pattern Recognition For Dip Calculations

In 1977, Schlumberger developed a dipmeter program that used pattern recognition instead of cross correlation to find dip angle and direction. The aim of the program, called GEODIP, was to reproduce, as much as possible, the ability of the human eye to recognize and match similar details on curves which are usually, but not necessarily, nearly identical. Dresser Atlas offers a program called STRATADIP which is similar in concept to GEODIP.

The following description was paraphrased from An Approach to Detailed Dip Determination Using Correlation by Pattern Recognition, P. Vincent et al, SPE Paper 6823, 1977.

One of the objectives of GEODIP is to overcome the rigidity of the fixed correlation interval procedure and provide a density of information more closely related to the geological detail seen on cores. There was also the feeling that the dipmeter raw data contained more information than was actually being used, even by the improved processing achieved with clustering and pooling. After all, the electrodes had a resolution of 0.2 inches and often one or two foot data was being presented.

Many features, such as peaks and valleys, are identifiable by eye from curve to curve on the dipmeter. These features have various thicknesses (from one inch to several feet), amplitudes, and shapes. Each feature may be considered to be the signature of a geological event in the depositional sequence. Moreover, the dip of the bedding is not necessarily constant, and may sometimes vary rapidly. The method of correlation by pattern recognition is best adapted to automatically detect these curve features, to recognize them from curve to curve, and to derive dips for the boundaries of each individual feature.

Different curve features of the same type are often very similar and easy to confuse. The human correlator avoids this ambiguity by constant eye movements to confirm or invalidate hypothetical correlations. In so doing, the correlator implicitly, often unconsciously, applies some logic rules which are integrated into the perception process. In the GEODIP method, equivalents of such rules and safeguards are included, as far as they have been recognized, in the program logic. Programs of this type have been called expert systems, or knowledge based systems, because they contain the rules of experienced analysts.

The method is constructed around a basic law justified by geological conditions of deposition, the rule of noncrossing correlations. This rule states that the layers are deposited one over another, so that they can wedge out but they cannot cross. The consequence is that if Event A appears above Event B on one curve, it cannot appear below B on another one. This rule induces a certain interdependence between all of the correlations. In this method, the correlations are not viewed as independent realities, but as parts of a more general structure having internal organization and rules.

Where only two curves are considered, it is a simple matter to recognize crossover correlations and disregard them. But when more than two curves are involved, as in Figure 5.28, complex logic is required within the computer program to perceive that the correlation (A1, A2), is inconsistent with the correlations (B1, B3) and (C2, C3). Actually, it is the set of the three

correlations which is, as a whole, inconsistent. It cannot be inferred, from what is shown, which one is incorrect.

The goal of the computer logic is to select the largest set of curve to curve correlations that does not include any crossovers or implied crossovers. To meet this goal, a branch of modern mathematics called the theory of partially ordered sets has been applied to the description and consistency checking of sets of correlations between curves. While this theory is necessary to properly implement on a computer the rule of noncrossing correlations, an understanding of the mathematics is not needed to appreciate what it achieves.

The method of correlation by pattern recognition is composed of two main phases:

1. feature extraction (detection of curve elements)
2. correlation between similar features

In phase one, each curve is analyzed individually with reference to a catalog of standard patterns or types of curve elements, such as peaks, troughs, spikes, and steps, and is decomposed into a sequence of such elements. At the end of the feature extraction phase, the curves are replaced by their description in terms of elements.

Each element is associated with one or two boundaries which give the position of the element on the initial curve as well as a pattern vector, which is a series of numbers characterizing the shape of the element. The pattern vector for a peak contains a description of its:

1. average (P1)
2. maximum (P2)
3. position of maximum, X_m , relative to boundaries, B1 and B2,
given by $P3 = (X_m - X1)/(X2 - X1)$
4. maximum minus average (P4)
5. balance left/right inflection point smoothed derivative
values ($d1$ and $d2$), given by $P5 = -(d1/d2)/(1+d1/d2)$
6. left jump (P6)
7. right jump (P7)
8. balance left/right jump, given by $P8 = -(P6/P7)/(1+P6/P7)$
9. width of peak (P9)

Other features have their own unique list of parameters in their pattern vector.

In the correlation phase, the method tries to successively match elements of one curve to similar elements of the others. The objective is to recognize the same geological event as it appears on different curves. The basic criterion is the comparison of pattern vectors. To find these correlations, a coefficient is computed which is a measurement of the likeness between any two elements, using the following equation:

$$L = \text{SUM } ((P_{ai} - P_{bi})^2)$$

L = likeness coefficient

P_{ai} = i th parameter for an element in curve A
 P_{bi} = i th parameter for a similar type element in curve B

Low values for L mean a high degree of likeness.

Then, the procedure attempts successive correlations according to a built in order of precedence: large troughs, then large peaks, then medium troughs,... The program retains already accepted higher precedence correlations in order to forbid crossing them in further attempts with correlations of lower rank.

When two elements are considered to be a match, the corresponding upper and/or lower boundaries are then correlated. The resulting dips are computed from the displacements measured between these correlated boundaries and not those measured between the elements themselves.

At the beginning of the correlation phase, an initial search angle, corresponding usually to the highest value of expected dip magnitude, is imposed. The initial search distance is computed from the input search angle, the orientation parameters, and the diameters measured by the tool at the particular level. As correlations are made and accepted, the search distances are modified, as necessary, to avoid crossing correlations.

It may happen that no large element can be correlated with any large element of the same type on the search curve. To handle these cases in following passes, requirements are relaxed, for instance, by authorizing the correlation of a large element of the base curve with a medium element of the same type on the search curve. On the other hand, the correlation of unlike elements, such as peaks with troughs, is forbidden.

Thus, the correlation phase proceeds by successive passes, searching first for the most obvious correlations, those having the lowest likeness coefficients. Each time a correlation is retained, it is memorized in order to limit subsequent search lengths for correlations with higher likeness coefficients.

Pattern recognition correlation is also used in determining the velocity correction, allowing almost inch-by-inch detection of speed variations.

Figure 5.29 shows the graphic presentation made by automatic plotter. Because of the large number of dip results found, a depth scale of 1/40 (30 in. per 100 ft.) or 1/24 (50 in. per 100 ft.) is used instead of the usual 1/240 or 1/200 scales. This uncommon depth scale is better adapted for the high resolution available for very thin beds. The semihorizontal lines connecting the traces represent the correlation of element boundaries. Figure 5.30 shows a typical listing from this program.

With GEODIP there is no quality rating of the dip determination. The visual display of the curves and the correlations enable analysts to decide for themselves about the reliability of the correlations according to the character of the curves. Comparison to core data is one way to check the validity of the results of stratigraphic analysis. Figure 5.31 illustrates one such comparison.

Stratigraphic High Resolution Dip Calculations

From the above discussion, it is apparent that a program that combined both structural information as in pooled clusters and stratigraphic correlations as in GEODIP would be a good idea. The SHDT and its companion computation program, DUALDIP, provide this, with three independent computations of formation dip. This allows the possibility of adapting the interpretation to the specific problem of interest, whether structural, sedimentary, or sand body geometry. SHDT and DUALDIP are Schlumberger trademarks. The three calculation modes described below were extracted from Applications of the SHDT Stratigraphic High Resolution Dipmeter, Yves Chauvel et al, Trans SPWLA, 1984.

1. MSD Dips (Mean Squares)

These result from all the possible cross correlations between couples of sensors, giving up to 28 curve displacements at each level. The correlations are done in the standard way, and require definition of correlation length, step distance, and search angle. A plane is then fitted through all the available results, using a repetitive logic of discarding the most distant displacements and then refitting. This results in either:

- a good quality dip (full arrowhead) if distances from mean are small and few displacements are discarded.
- a low quality dip (open arrowhead) or no dip at all, if distances from mean are large and/or many displacements are discarded.

There is no vertical continuity logic or clustering routine in the MSD computation, and each level is autonomously processed. The clustering is thus replaced by an analysis of the local scattering of the displacements. This method benefits from the ample redundancy available from 28 displacements, while two would be enough to define a dip, reducing the possibility of producing random dips or noise correlations.

2. CSB Dips (Continuous Side-by-Side)

While the MSD dips respond to major geological events, the CSB focuses on fine details very much like a geologist studies the sedimentation of a sequence through the inspection of a core. Each pair of twin curves (eg. electrodes 1 and 1A) is cross correlated on a fine interval (typically, 12" x 3"). This gives a vector parallel to the dip plane. Another vector is found at the same depth by cross correlation of an adjacent pair of twin curves (eg. 2-2A). Taken together, the two vectors define a dip plane. The CSB dips will be as dense as the step length chosen permits (eg. up to 4 per foot for a 12" x 3" computation).

With only four side-by-side correlations, the only cross check available is to verify that, for a planar bed, the displacements obtained from opposite pairs of curves (eg. 1-1A and 3-3A) should be equal in value and opposite in sign.

This occurs if closure error is zero. If this is the case, any combination of these displacements yields the same dip and any orthogonal pair is used to produce the dip at that depth. If this is not the case, a window is opened around the level under examination, and the vertical continuity of the displacements within the window is checked. The orthogonal pair showing the smoothest continuity within the window is selected for dip computation.

Whether a good quality dip (full arrowhead), a low quality dip (open arrowhead), or no dip is output, is a function of the quality of the side-by-side correlations established and of the vertical continuity of the displacements.

3. LOC Dips (Local Derivative)

An event detection logic is used on the eight curves to establish pinpoint correlations between events on the curves. As in GEODIP, the computer processing uses a derivative filter to obtain absolute dips independent of dips at other depths, similar to what could be found by manual correlation. There are however a few differences.

To be retained as a LOC dip, an event has to be recognized on at least 7 of the 8 curves, while the GEODIP logic requires only 3 out of the 4 curves. Thus the LOC dip logic is more demanding than the GEODIP logic, which explains why generally fewer LOC dips are obtained than GEODIP results on comparison runs.

The LOC dips are further refined by a cross correlation made on a 12" interval, while GEODIP results are computed directly from the spot events on the curves. This cross correlation involves the eight curves and includes a repetitive best fit and rejection logic as in the MSD computation, with similar criteria for quality coding (full or open arrowhead).

A measurement of the planarity is derived from each of the possible dip planes at any level. The retained value corresponds to the surface which best approximates the set of these planes. By convention, a perfectly planar surface has a planarity of 100.

Some events are recognized on only some of the dip curves. In this case, the available correlations are traced across the applicable curves, with an optional notation of "F" (Fracture) or of "P/L" (Pebble/Lens) for single pad events or two/three pad events, respectively. These interpretations, however, are not to be considered as certain, but rather as possible.

Due to their origin (pad-to-pad correlations), the LOC dips have meaningful lateral significance. If structural dip is present, it will normally be seen by the LOC dips rather than by the CSB dips. Generally the statistical agreement between the LOC and the MSD dips can be expected to be quite good.

DUALDIP is the computer program which produces the standard SHDT result presentation. This includes CSB and LOC dips, the eight dip curves, the synthetic resistivity and gamma ray curves, calipers and hole drift data. The depth scale is usually 1/40, and as an option the MSD dips can be added to this output. A sample was shown earlier as Figure 5.16.

Structural interpretation is done using the MSD dips. Due to the logic used, namely cross correlation made using long intervals, the MSD dips are the ones likely to represent laterally significant and vertically consistent geological events. For optimum use of the MSD dips, a reduced scale (1/200) plot is normally produced. This plot is also the single SHDT product when no fine scale studies are contemplated.

The prime objective of the SHDT tool design is to improve the ability to provide reliable answers to sedimentary interpretation problems. While the rules of interpretation remain essentially the same as in HDT interpretation, there are additional possibilities. Among the information that can be retrieved by visual analysis of the dip curves, reconstructed resistivity, and dip arrows are:

- type of lithology (shale, sand, conglomerate) from the shape and likeness of the curves.
- fining upwards, coarsening upwards sequences. This is done by analysing the resistivity variations across the sequence, either with the dip curves themselves or with the synthetic resistivity curve. Other open hole logs, such as the gamma ray (combinable with SHDT), are useful here. Care should be exercised using the resistivity, however, since fluid saturations have to be accounted for when inferring grain size variations from resistivity gradients.
- homogeneous bodies (no apparent bedding) as opposed to finely striated, laminated bodies.
- parallel vs nonparallel bedding. This is especially important in sandstones, and has found recent applications to the study of turbidites.
- correlation lines: some correlations involve the eight resistivity curves, some do not. The most appropriate interpretation (pebble, lens, fracture, other) will be made on the basis of the dip curves (conductive or resistive anomaly, number of pads involved, etc.).
- fractures: open fractures will show as isolated conductive spikes which may or may not correlate with similar spikes on other dip curves.

Some of the important uses of the CSB dips are:

- determination of bedding angle and direction in those (frequent) cases where they do not show as MSD (or LOC) dips. This is the case, for example, in coarse grained sandstones where bedding is only indicated by minute changes of resistivity, and not by the existence of large contrasts. This is also very common in evaporitic sequences.
- determination of the direction of sediment transport, a corollary to the above. This is especially interesting in severe cases of cross bedding, when the only dips produced by long interval correlations generally correspond to those of the individual sedimentary units, seen at their interfaces, and not to the actual current bedding surfaces.

- conventional sedimentary interpretation (red, blue patterns, direction of sand body thickening, etc.). All of this can be done on an almost microscopic scale.
- CSB dips are also very useful, and often better than MSD dips, in high angle apparent dips, when longer correlation intervals are used.

LOC dips can be used to study such features as:

- nonparallel bedding, for example, when the upper and the lower boundaries of thin beds do not have the same dip. In cases of poor planarity, the event recognition logic will be too tight for a LOC dip to be produced, and the MSD curves may then provide the answer. This is particularly important if this bed is to be found in another well, or when looking for the direction of updip or downdip thickening.
- cross bedding: the LOC dips will see the interfaces between the individual sedimentary units, when apparent. This dip may not coincide with the angle and direction of deposition in cross bedded formations (eg. tabular bedding, foreset beds).
- turbulence of deposition, when causing nonplanarity of bedding.

The MSD dips are normally not used for sedimentary studies, being the result of an averaging of the dip curve anomalies over the length of the correlation interval. They are usually presented on the DUALDIP plots, however, for structural reference. The vertical (depth) scale used for stratigraphic work makes it difficult to see structural patterns in the MSD data.

Acknowledgements

I would like to thank John Cox for his helpful review of this chapter, and for his unflagging assistance over the years as the dipmeter guru of Canada.

About The Author

E.R. (Ross) Crain, P.Eng. is proprietor and chief consultant, Spectrum 2000 Mindware Ltd., and has spent 28 years in exploration and production geology, well logging, seismic data processing, reservoir engineering and description, micro and mainframe computer applications, and business management. His principal activities include consulting on a wide range of well log and microcomputer related topics; presentation of courses and seminars on formation evaluation; development of fourth generation (spreadsheet) and fifth generation (knowledge based) software for desktop work stations for the oil and gas and the agricultural community.



THE LOG ANALYSIS HANDBOOK

FIGURE 5.01: THREE ARM DIPMETER

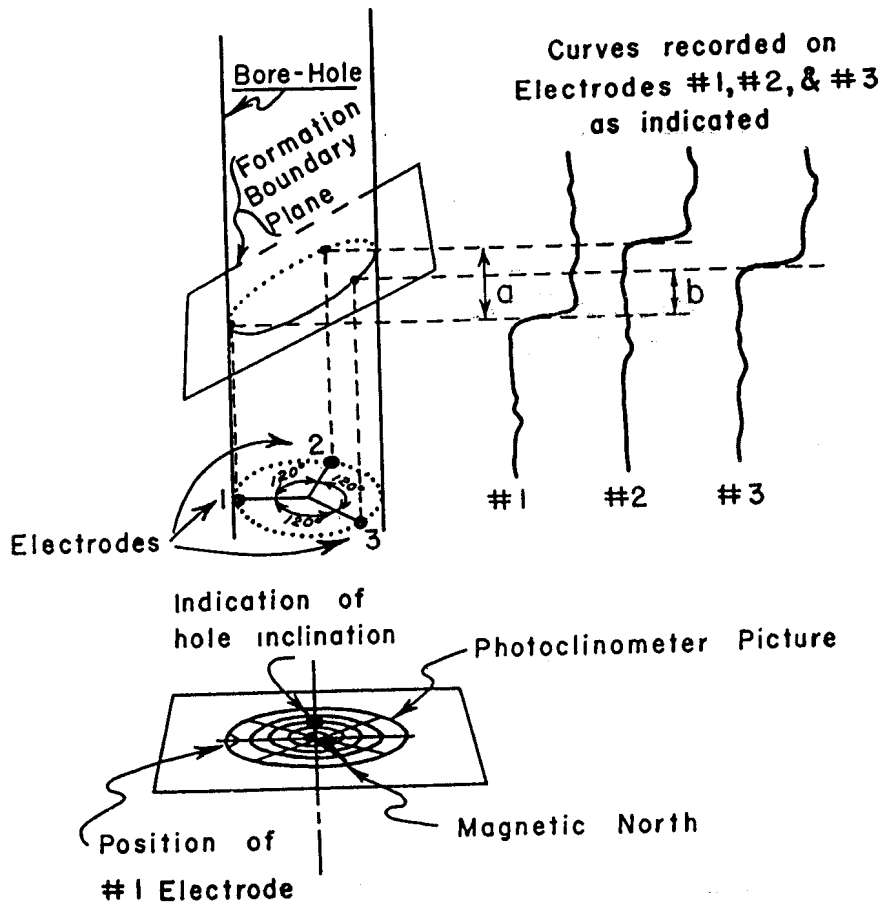

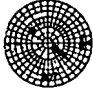







Illustration courtesy of Schlumberger

THE LOG ANALYSIS HANDBOOK

FIGURE 5.02: PHOTOCLINOMETER PLOT

DEPTH	DIFT ANGLE	BEARING	
10,400	3°45'	180°	
10,500	3°45'	181°	
10,600	3°45'	182°	
10,700	4°00'	183°	
10,800	4°00'	181°	
10,900	4°00'	181°	
11,000	4°15'	181°	

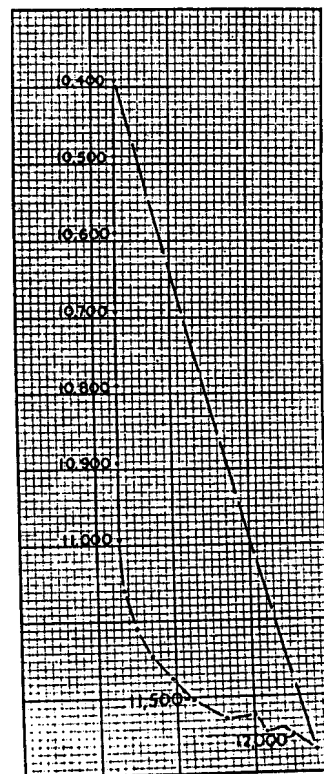


Illustration courtesy of Schlumberger

THE LOG ANALYSIS HANDBOOK

FIGURE 5.03: DIRECTIONAL SURVEY

FORM 142.0

SCHLUMBERGER WELL SURVEYING CORP. PHOTOCLINOMETER SURVEY												
COMPANY: FIELD:					WELL: DATE:							
DEPTH	DRIFT ANGLE	DEFLECTION			LATITUDE		DEPARTURE		COORDINATES			
		TRUE BEARING	HORIZONTAL FOOTAGE	VERTICAL FOOTAGE	N	S	E	W	N	S	E	W
Casing shoe at 2000'												
2100	0°30'	S 54 E	.87	100.00		.51	.71			.51	.71	
2300	0°15'	N 45 E	.87	200.00	.62		.62		.11		1.33	
2500	0°15'	N 36 W	.87	200.00	.71			.51	.82		.82	
2700	0°15'	N 70 E	.87	200.00	.29		.82		1.11		1.64	
2900	0°15'	N 2 E	.87	200.00	.87		.03		1.98		1.67	
3100	0°0'	-	0	200.00					1.98		1.67	
3300	0°15'	N 49 W	.87	200.00	.57			.66	2.55		1.01	
3500	0°15'	N 16 W	.87	200.00	.84			.24	3.39		.77	
3700	0°15'	N 8 W	.87	200.00	.86			.12	4.25		.65	
3900	0°0'	-	0	200.00					4.25		.65	
4100	0°15'	N 41 W	.87	200.00	.66			.57	4.91		.08	
4300	0°30'	S 60 E	1.75	200.00		.86	1.51		4.05		1.59	
4500	1°0'	S 57 E	3.49	199.97		1.90	2.92		2.15		4.51	
4700	1°15'	S 60 E	4.36	199.95		2.18	3.78			.03	8.29	
4900	1°45'	S 63 E	6.11	199.91		2.77	5.44			2.80	13.73	
5100	2°0'	S 61 E	6.98	198.88		3.38	6.10			6.18	19.83	
5300	2°30'	S 53 E	10.90	249.76		6.56	8.71			12.74	28.54	
Total depth of hole at 5350'												

Illustration courtesy of Schlumberger

THE LOG ANALYSIS HANDBOOK

FIGURE 5.04: DIRECTIONAL SURVEY PLOT

FORM 224.2

SCHLUMBERGER WELL SURVEYING CORPORATION PHOTOCLINOMETER SURVEY

COMPANY: _____ COUNTY: _____
WELL: _____ STATE: _____
FIELD: _____ RUN NO.: _____
LOCATION: _____ DATE: _____

SCALE: 1" = 10'

POSITION OF BOTTOM OF HOLE: 31.3 feet S 66° E of casing shoe

ALL DIRECTIONS ARE TRUE NORTH

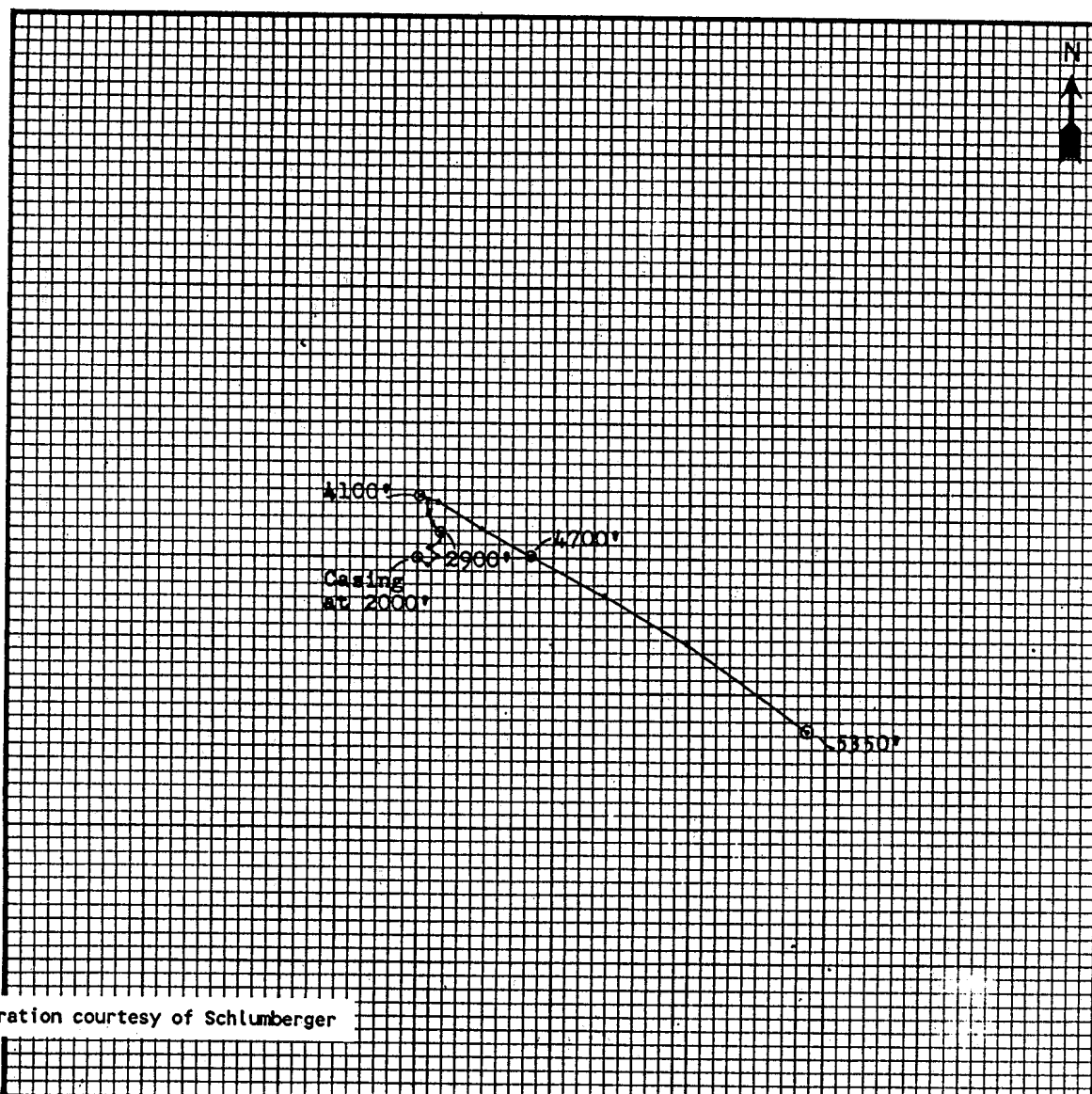


Illustration courtesy of Schlumberger

THE LOG ANALYSIS HANDBOOK

FIGURE 5.05: RAW DIPMETER PLOT - STATION BY STATION

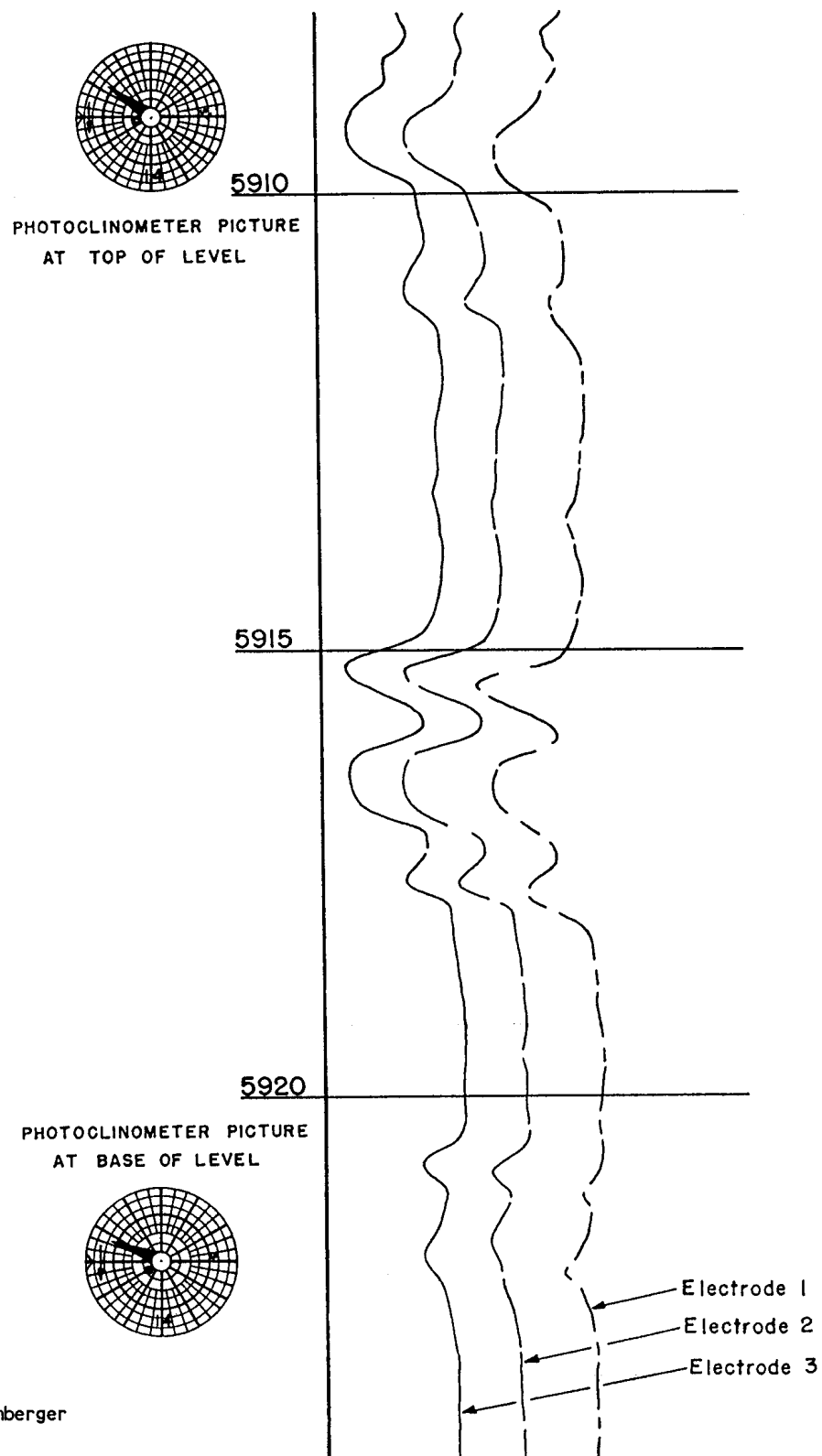


Illustration courtesy of Schlumberger

THE LOG ANALYSIS HANDBOOK

FIGURE 5.06: DIPMETER LISTING - STATION BY STATION

STA- TION	Depth Interval	From Magnetic North			Displacement of Curves in reference to I.		DIP			OBSERVATIONS
		Drift Azimuth	Drift Angle	Orient. No. I	II	III	Dip Angle	Mag. N.	Direction from True North	
A1	2000 to 2020	342	0 45	77	U 0.4	U 1.2	9	120	S 50 E	
A2	2004 to 2024	342	0 45	77	U 0.4	U 1.2	9	120	S 50 E	
B1	2856 to	234	2 00	229	D 0.6	D 2.2	17	91	S 79 E	
B2	2875	234	2 00	16	D 0.8	U 1.2	15	93	S 77 E	
C1	3135 to	241	1 00	119	U 1.8	U 0.6	13	75	N 85 E	
C2	3158	241	1 00	299	D 1.9	D 0.9	13	81	S 89 E	
D1	3520 to	237	2 00	214	-0-	D 1.8	15	88	S 82 E	
D2	3535	237	2 00	75	U 1.2	U 2.0	15	94	S 76 E	
E1	3608 to	238	2 15	292	D 0.8	D 2.2	14	140	S 30 E	
E2	3622	238	2 15	292	D 0.8	D 2.2	14	140	S 30 E	
F1	3844 to	242	2 00	265	D 2.0	D 1.2	15	60	N 70 E	
F2	3870	242	2 00	355	D 0.5	U 1.6	16	66	N 76 E	
G1	3990 to	242	2 15	312	D 2.0	-0-	17	66	N 76 E	
G2	4000	242	2 15	195	-0-	D 2.2	17	72	N 82 E	
	to									
	to									

FORM 188.0

SCHLUMBERGER WELL SURVEYING CORPORATION

Illustration courtesy of Schlumberger

THE LOG ANALYSIS HANDBOOK

FIGURE 5.07: DIPMETER ANSWER PLOT - STATION BY STATION

FORM 184.0					
STATION	Ref.	Depth Interval	DIP		
			Graph of Direction	Angle	Direction
			True North		from True North
A		2000 - 2024		9	S 50 E
B		2856 - 2875		16	S 78 E
C		3135 - 3158		13	N 88 E
D		3520 - 3535		15	S 79 E
E		3608 - 3622		14	S 30 E
F		3844 - 3870		15	N 73 E
G		3990 - 4000		17	N 79 E

CODE: —Heavy line shows direction of dip.
 —Cross-hatched sector between 2 thin lines indicates that direction of dip is anywhere within sector.
 —When station comprises two zones with different dips, dip for second zone is shown by broken (heavy or thin) line(s).
 —In Ref. Column, ES refers depths to electrical survey, DM to dipmeter log.

**SCHLUMBERGER
WELL
SURVEYING CORP.**

THE LOG ANALYSIS HANDBOOK

FIGURE 5:08: CONTINUOUS DIPMETER ANSWER PLOT

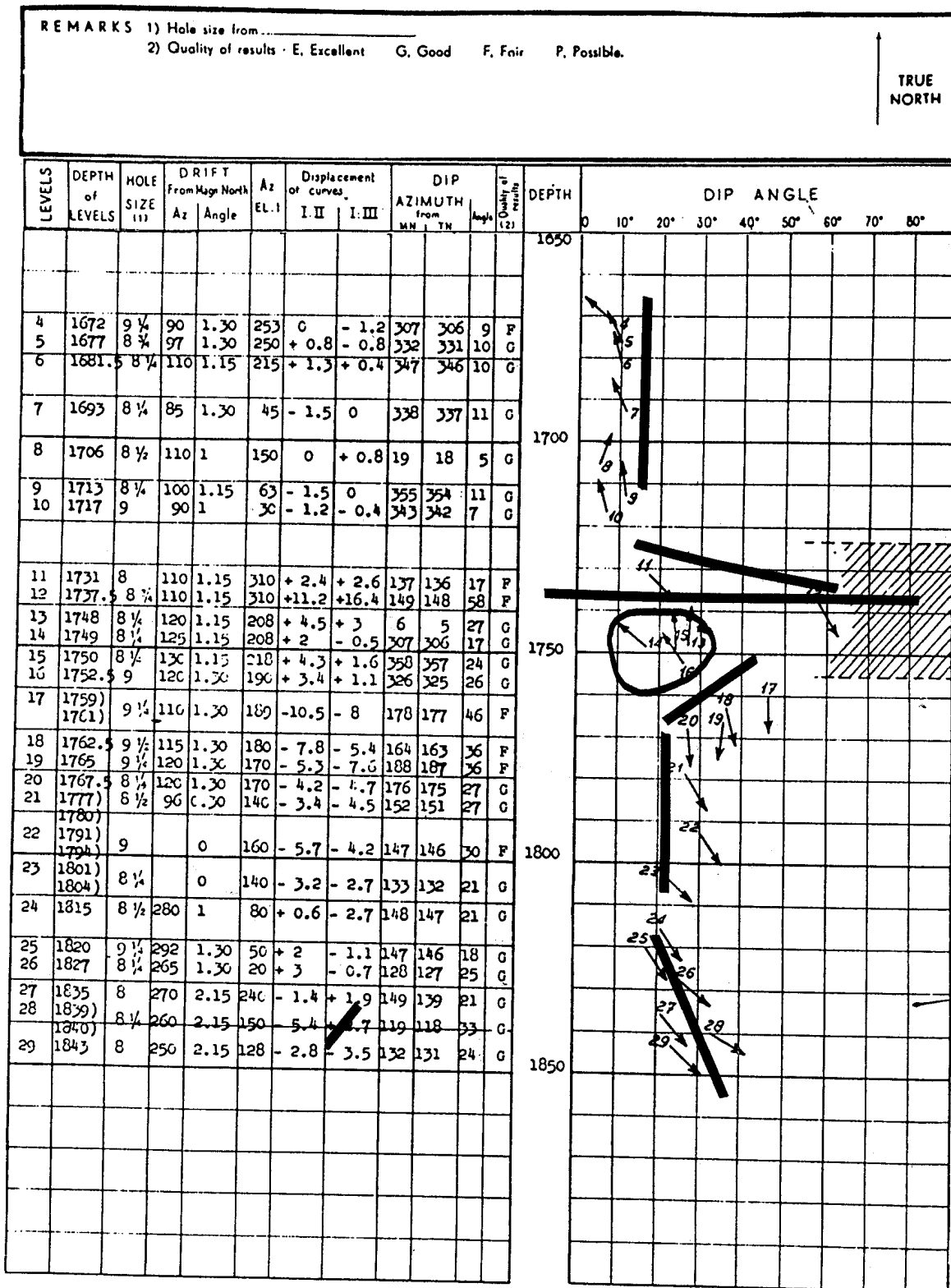


Illustration courtesy of Schlumberger

THE LOG ANALYSIS HANDBOOK

FIGURE 5.09: COMPARISON OF INTERVAL AND CONTINUOUS DIPMETER

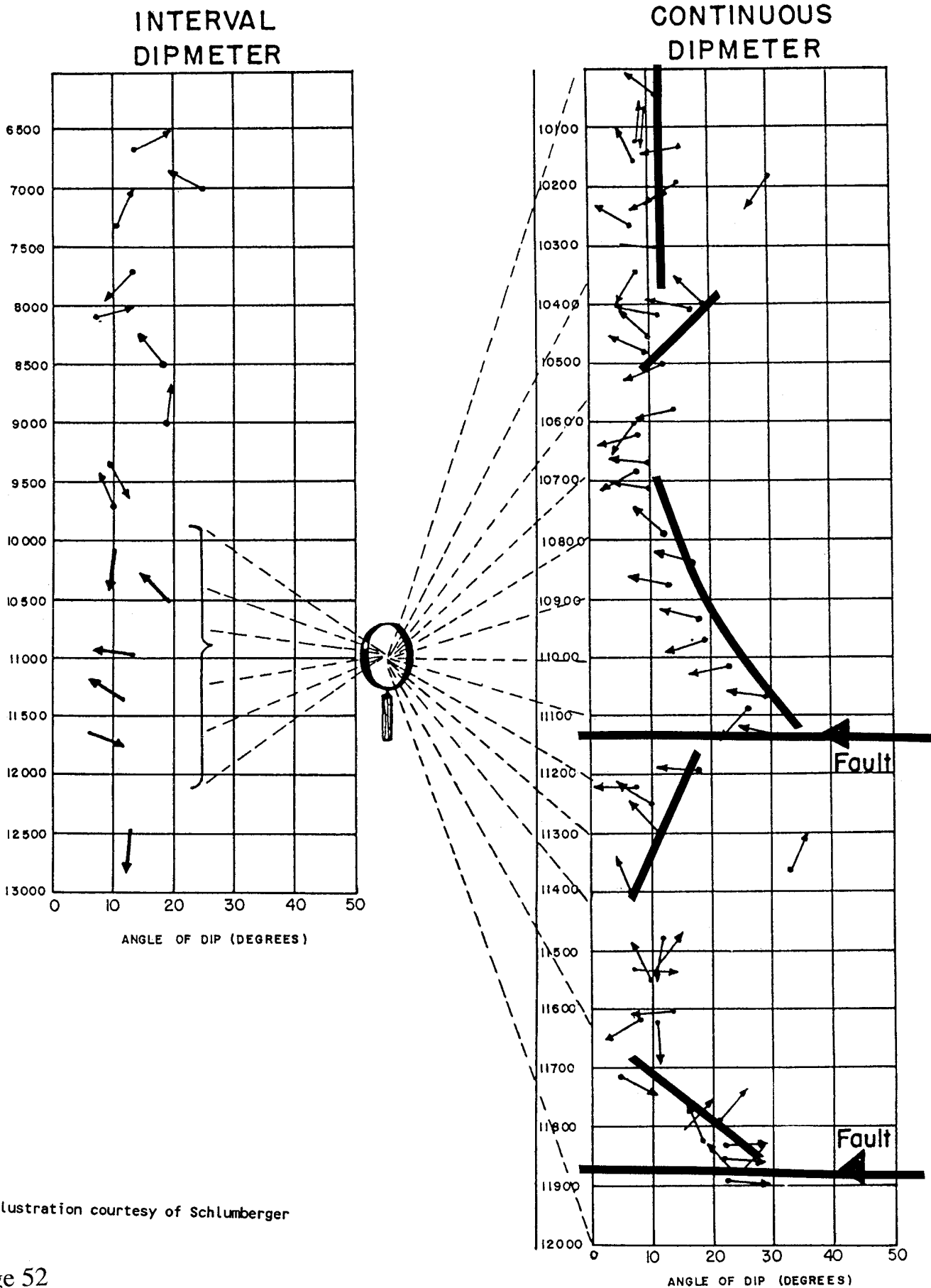


Illustration courtesy of Schlumberger

THE LOG ANALYSIS HANDBOOK

FIGURE 5.10: FOUR ARM DIPMETER - RAW DATA

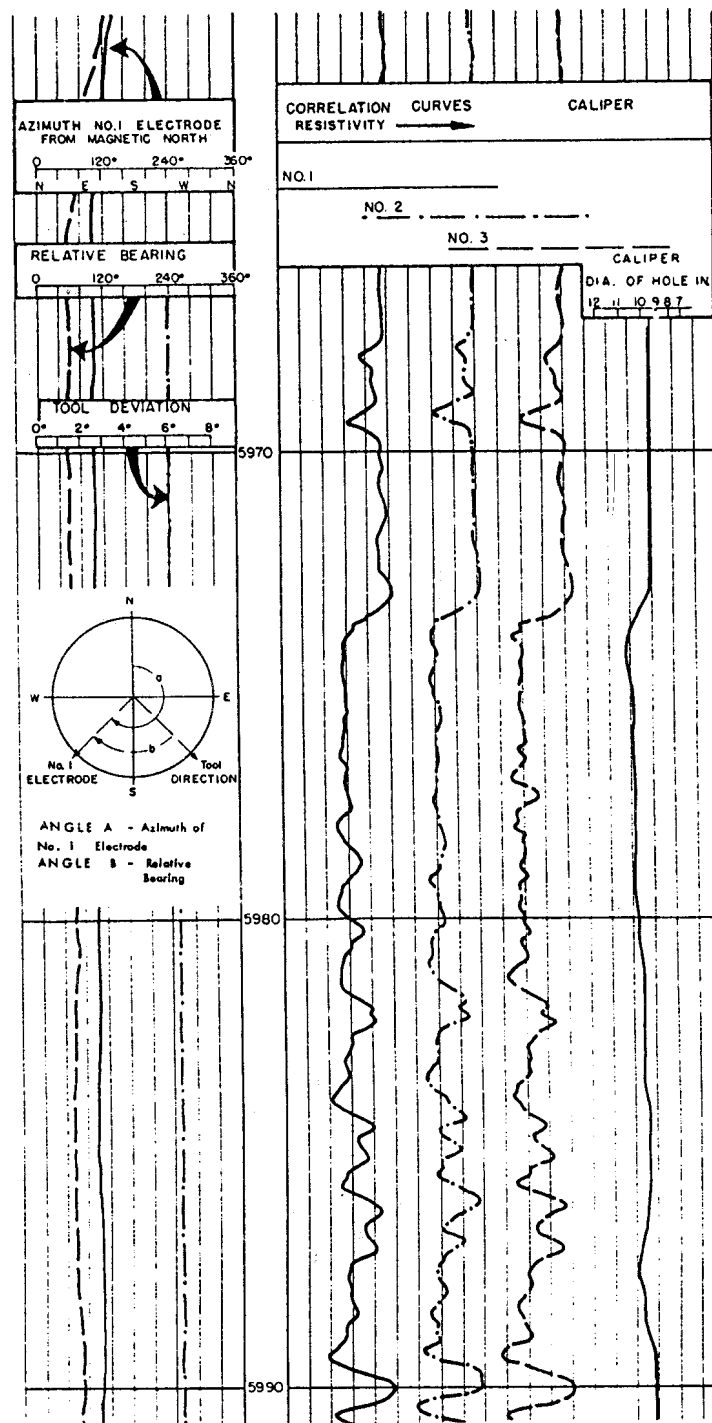
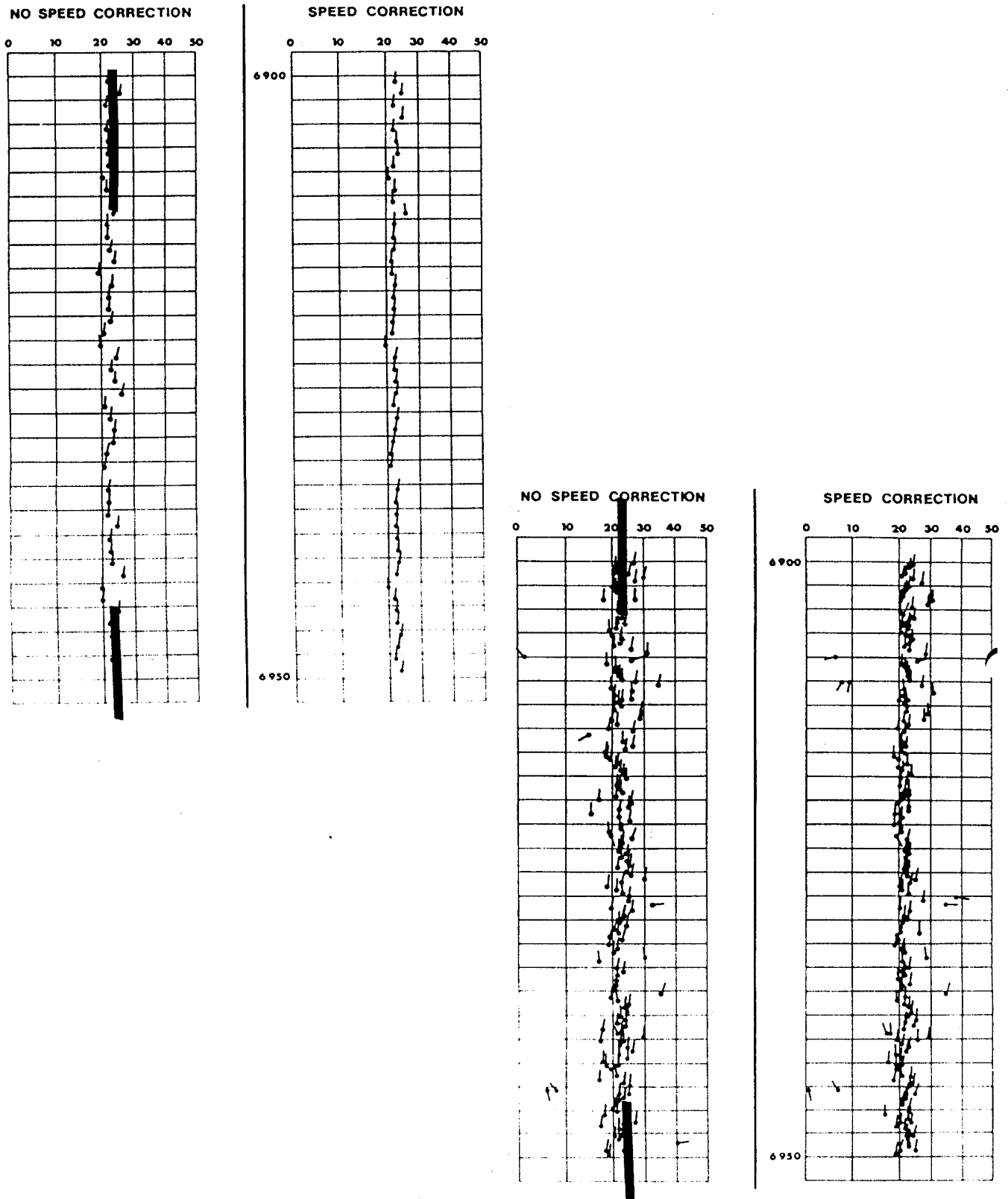


Illustration courtesy of Schlumberger

THE LOG ANALYSIS HANDBOOK

FIGURE 5.11: SPEED CORRECTION COMPARISON



From: High Resolution Dipmeter, Laud & Ringot, Log Analyst, May 1969

THE LOG ANALYSIS HANDBOOK

FIGURE 5.12: FOUR ARM DIPMETER DISPLACEMENTS

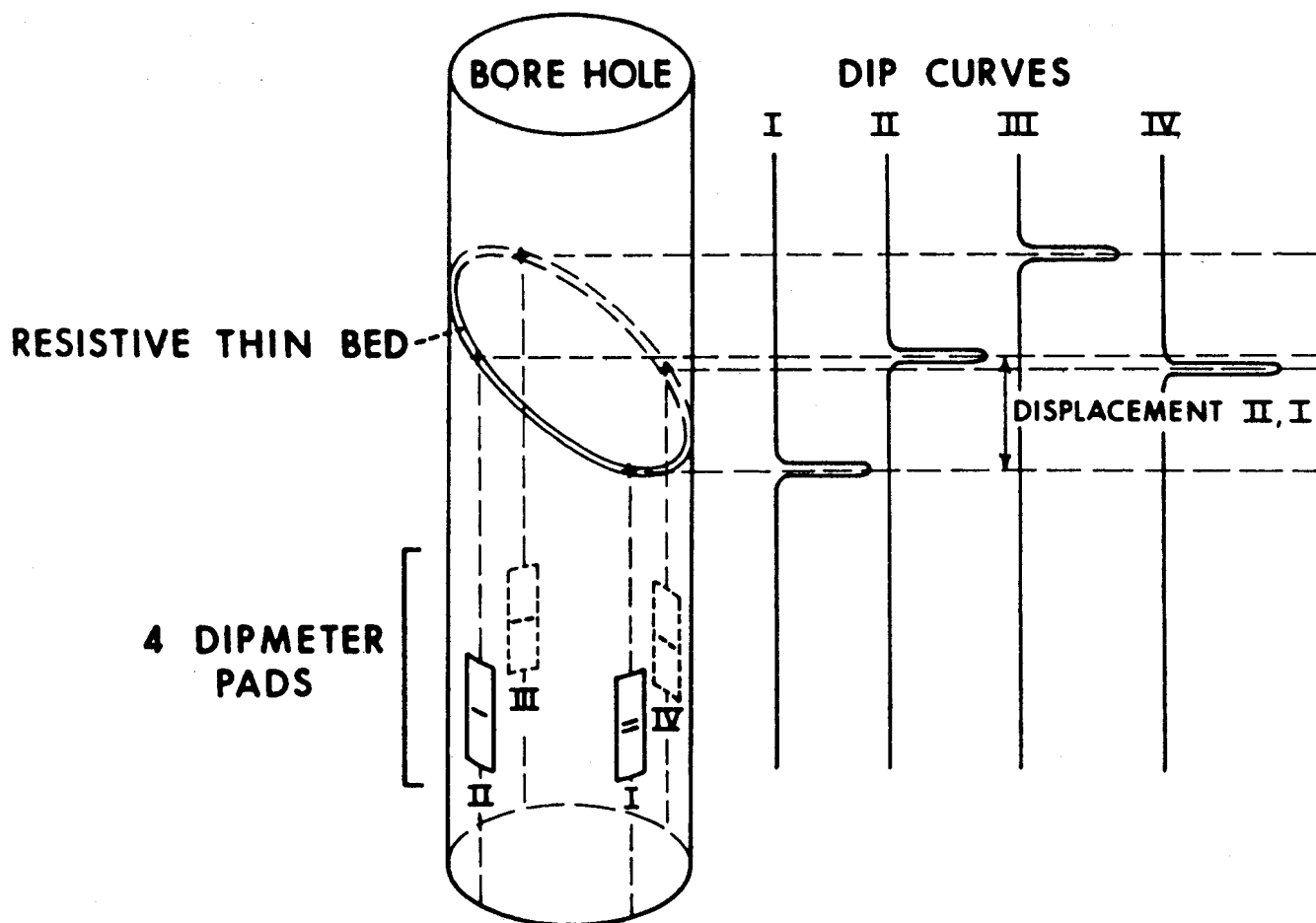
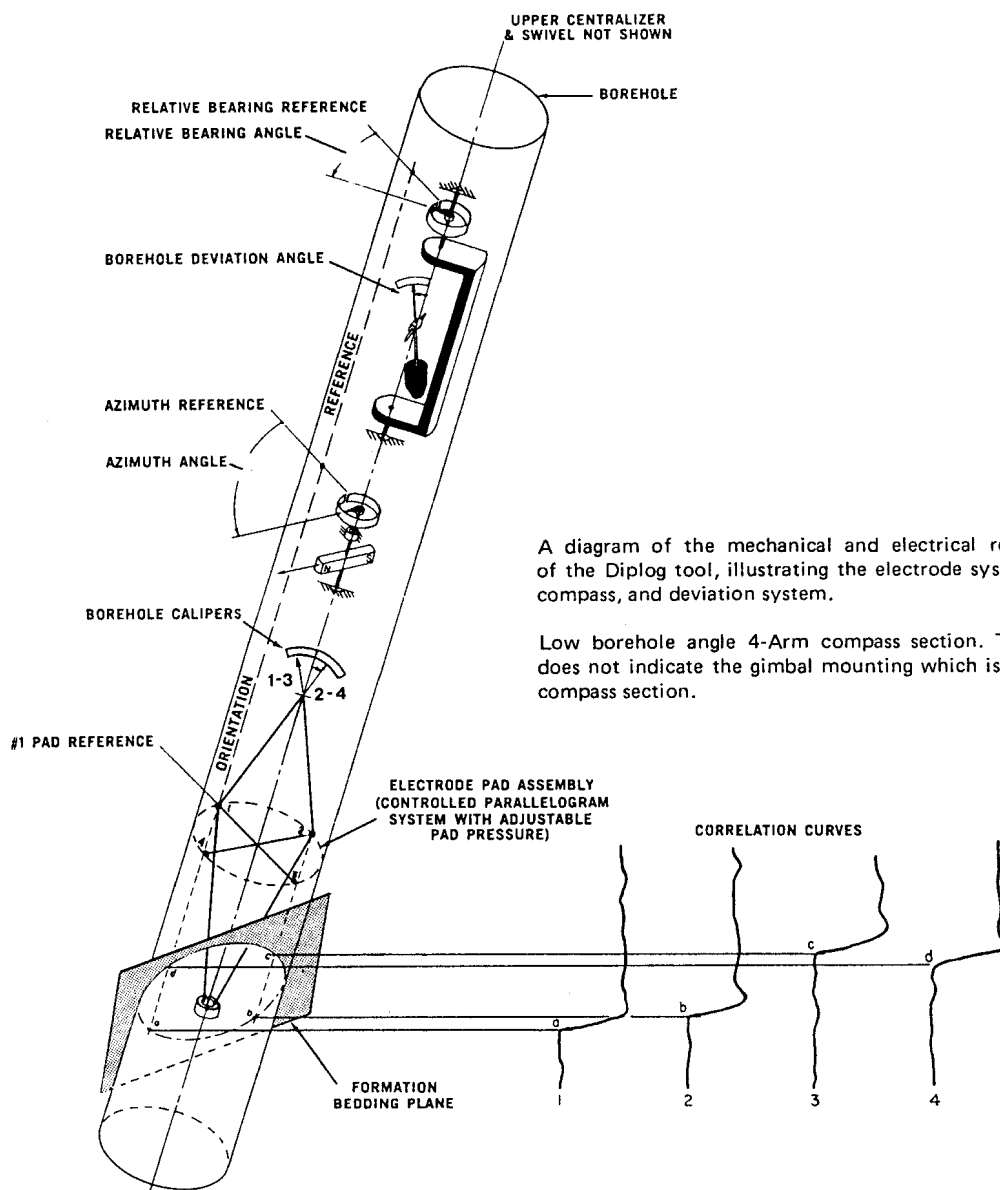


Illustration courtesy of Schlumberger

THE LOG ANALYSIS HANDBOOK

FIGURE 5.13: FOUR ARM DIPMETER TOOL



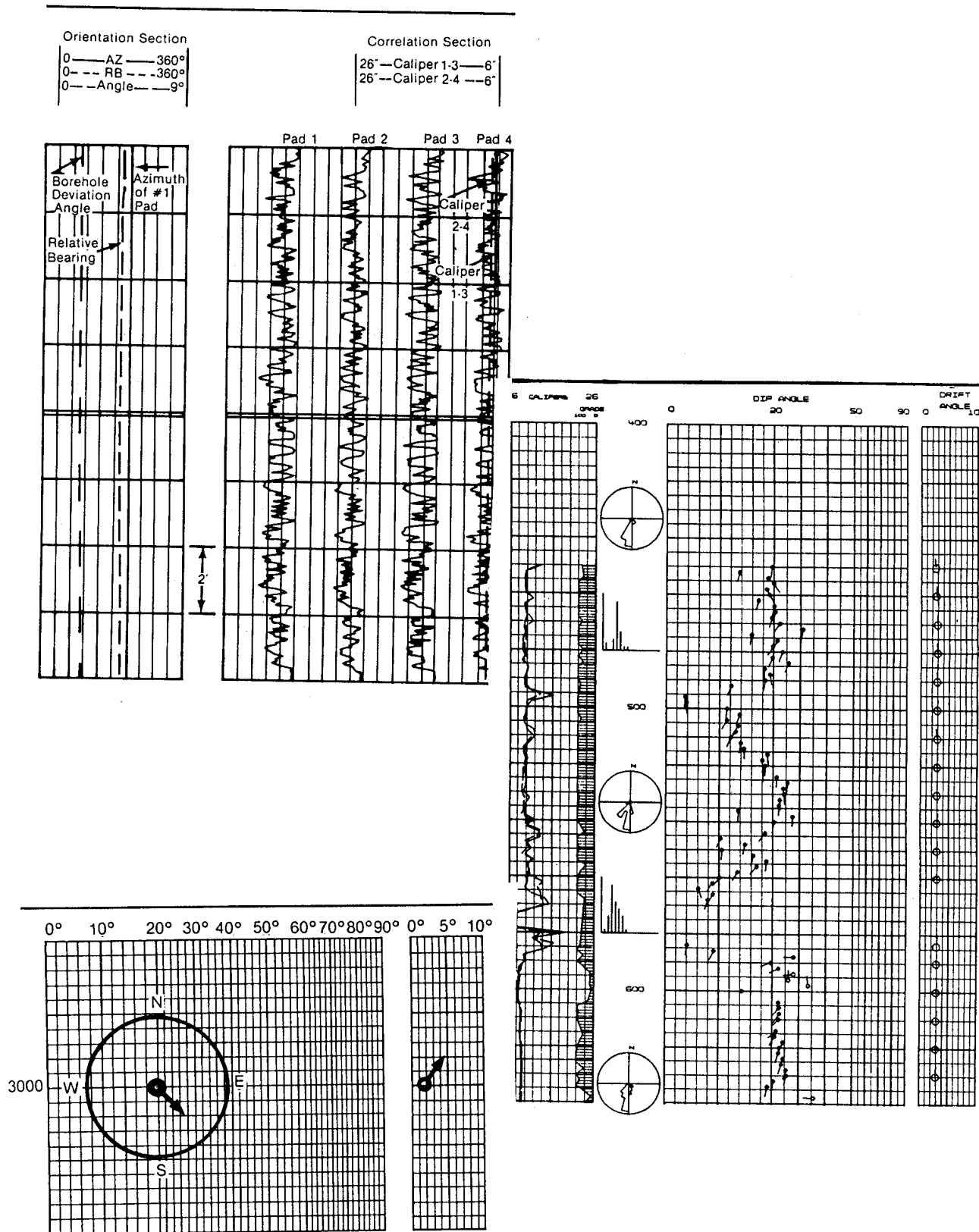
A diagram of the mechanical and electrical relationships of the Diplog tool, illustrating the electrode system, caliper, compass, and deviation system.

Low borehole angle 4-Arm compass section. This diagram does not indicate the gimbal mounting which is used on this compass section.

Illustration courtesy of Western Atlas

THE LOG ANALYSIS HANDBOOK

FIGURE 5.14: FOUR ARM DIPMETER ANSWER PLOT



Vector example. Vector at 3000 ft, dip 20° to the S., 40° E., azimuth 140°. Borehole is inclined 2° to the N., 45° E., azimuth 45°.

Illustration courtesy of Western Atlas

THE LOG ANALYSIS HANDBOOK

FIGURE 5.15: FOUR ARM, EIGHT BUTTON DIPMETER - RAW DATA

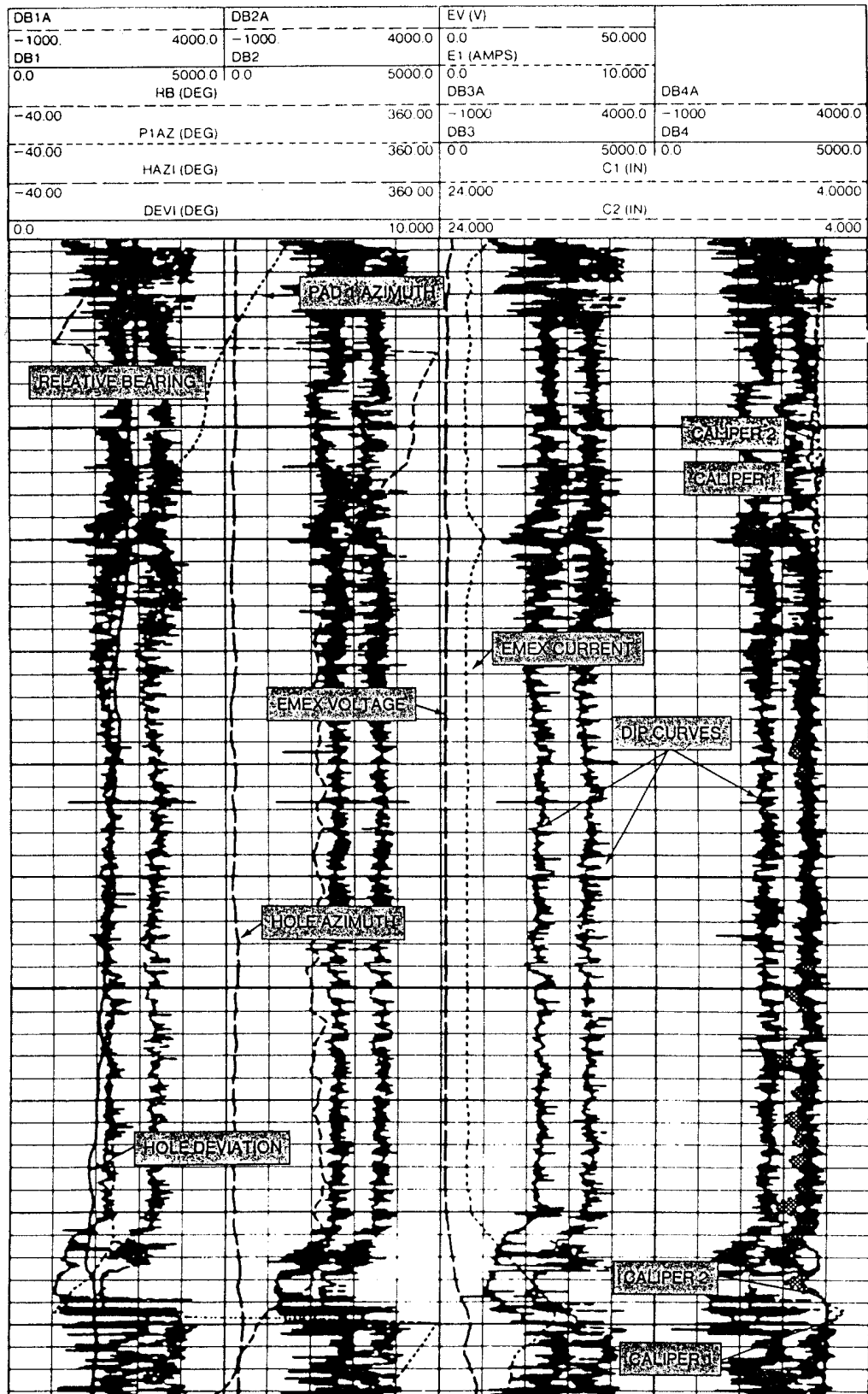
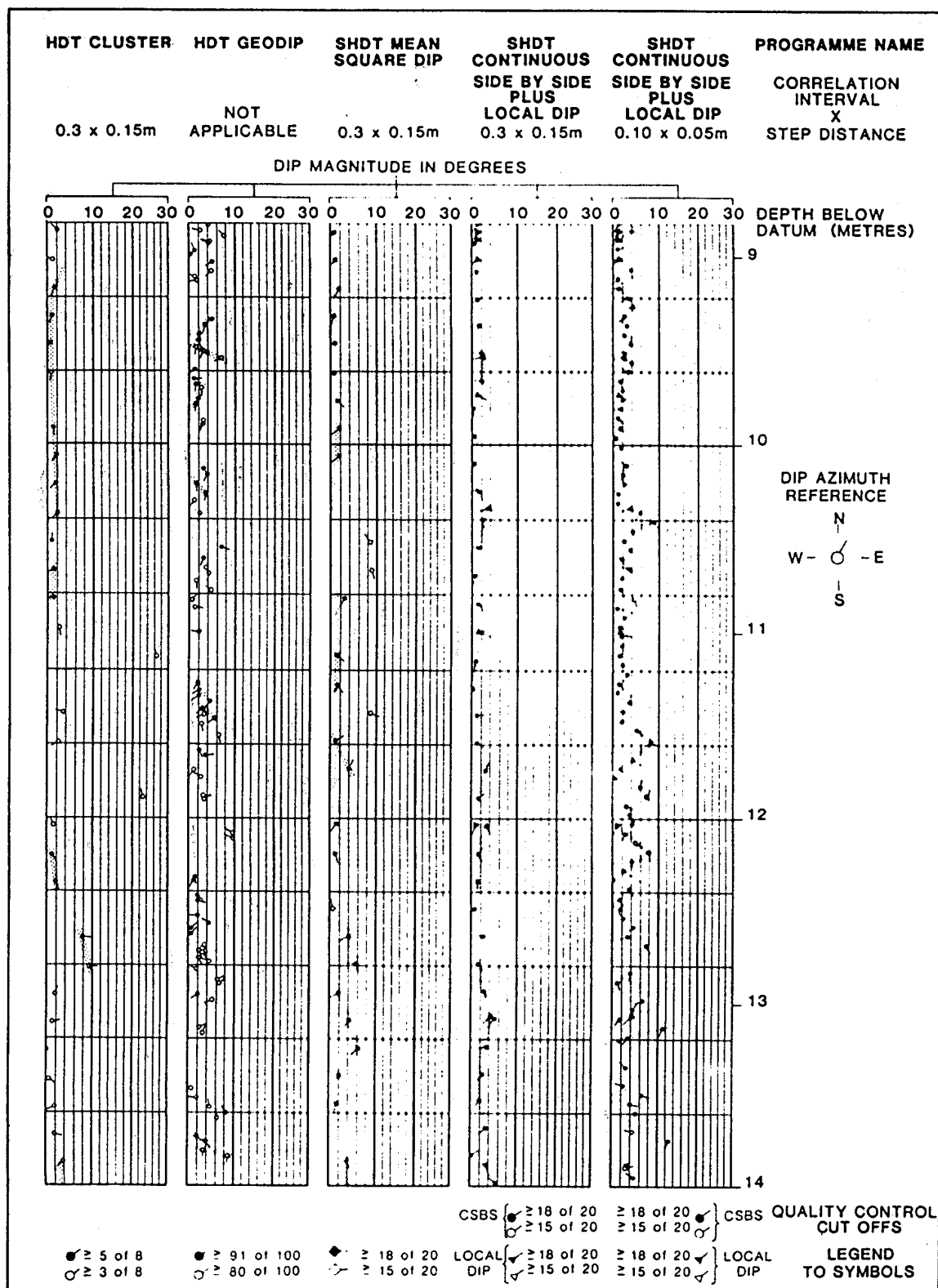


Illustration courtesy of Schlumberger

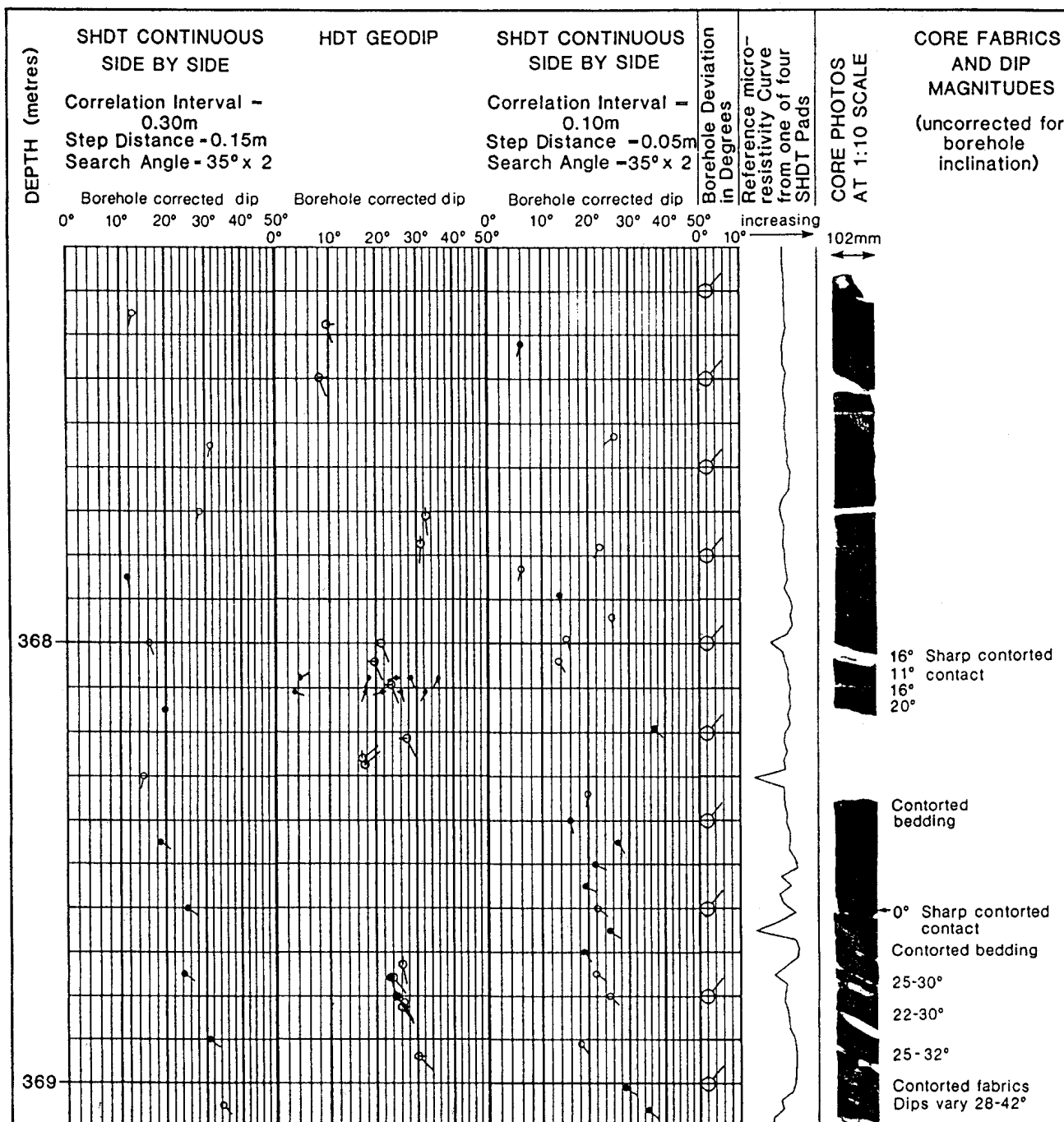
THE LOG ANALYSIS HANDBOOK

FIGURE 5.16: SHDT AND HDT COMPARISON



THE LOG ANALYSIS HANDBOOK

FIGURE 5.17: SHDT COMPARED TO CORE PHOTOGRAPH



From: Geological Interpretation of Alternate Dipmeter Analyses,
 B.A. Goldstein, Log Analyst, Nov 1986

THE LOG ANALYSIS HANDBOOK

FIGURE 5.18: FMS IMAGING AND SHDT DIPS

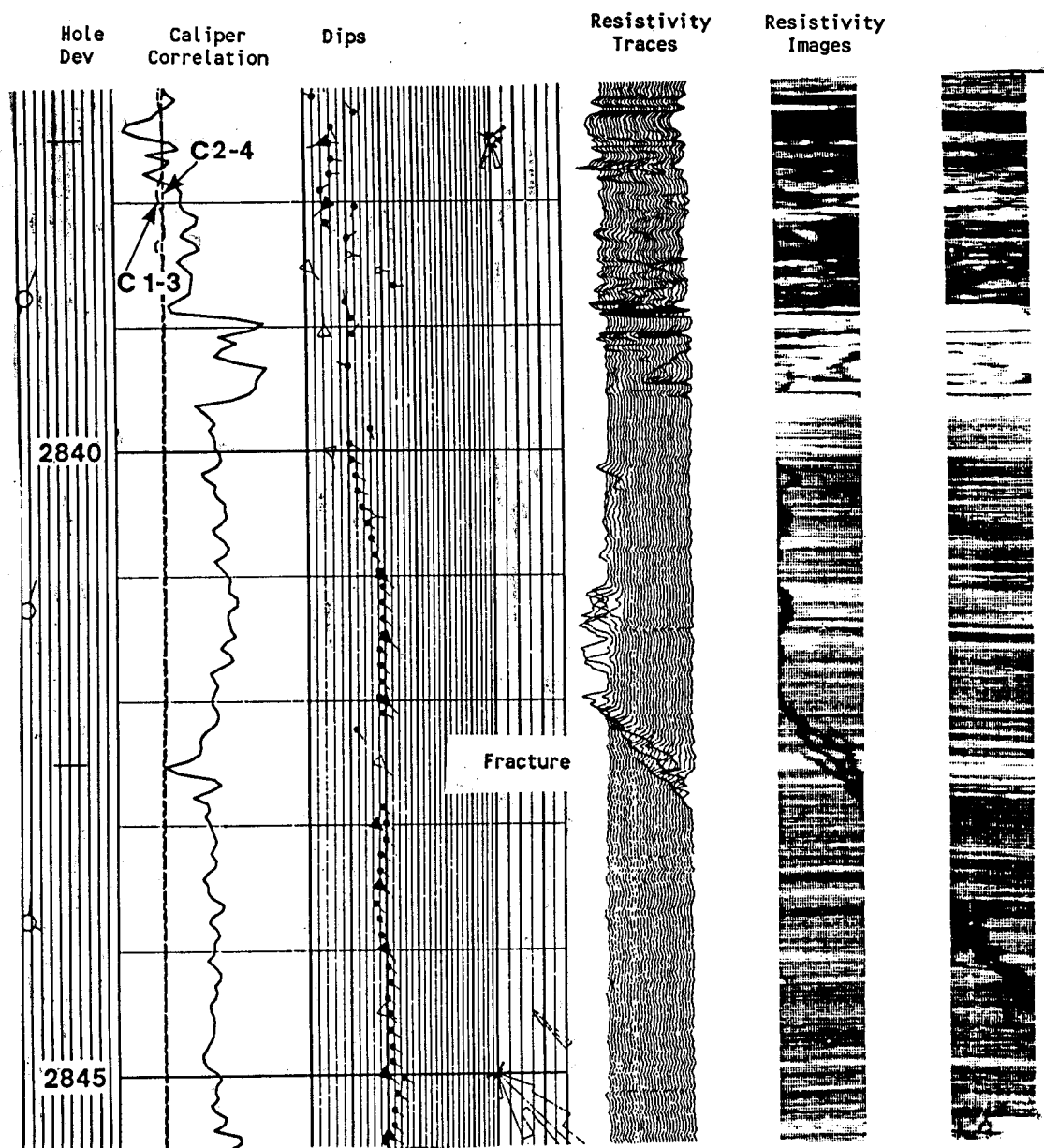


Illustration courtesy of Schlumberger

THE LOG ANALYSIS HANDBOOK

FIGURE 5.19A: COMPUTATION PARAMETER DEFINITIONS

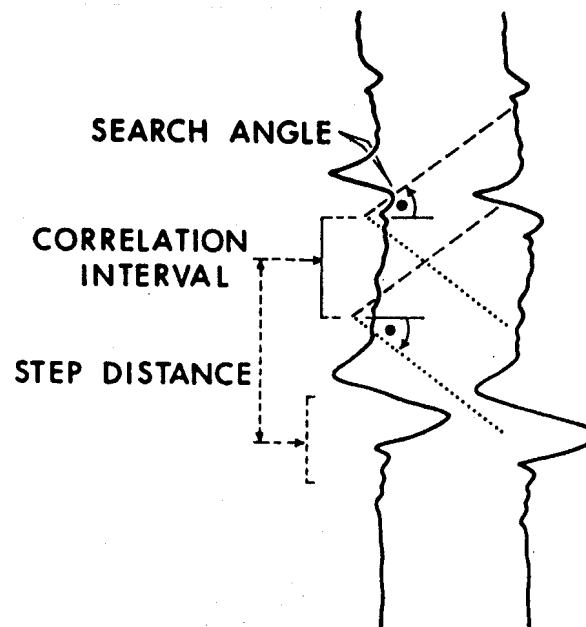


FIGURE 5.19B: LONG AND SHORT INTERVAL CORRELATION

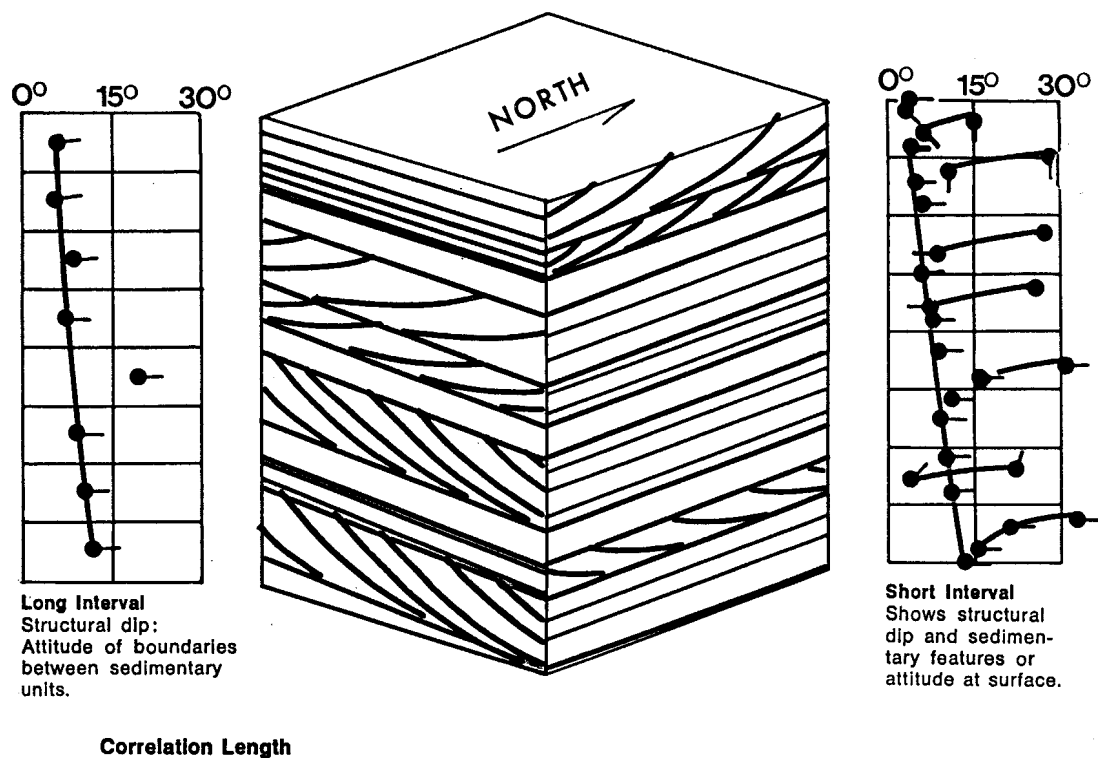


Illustration courtesy of Schlumberger

THE LOG ANALYSIS HANDBOOK

FIGURE 5.20: HDT PROCESSING FLOW CHART

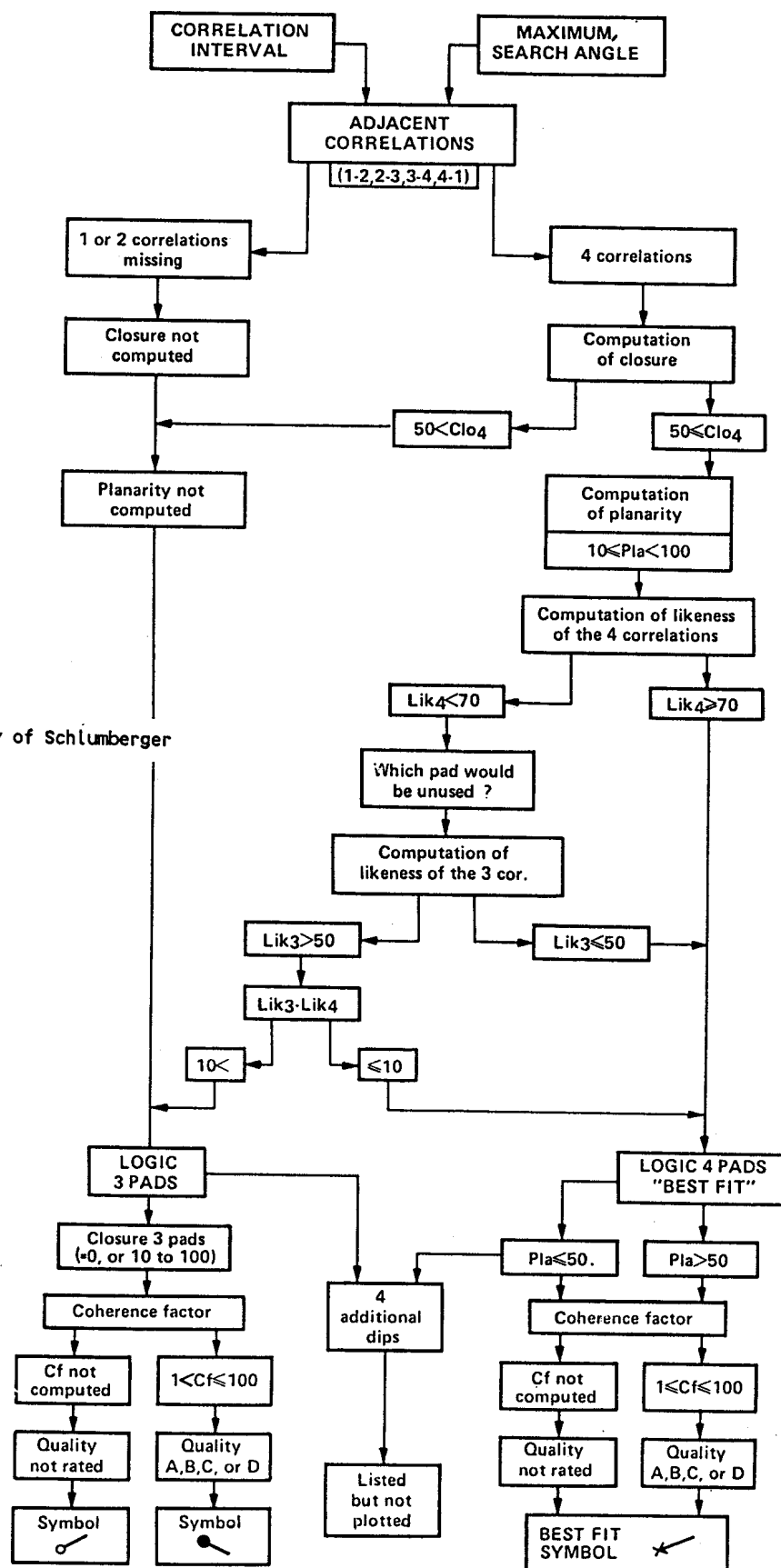


Illustration courtesy of Schlumberger

THE LOG ANALYSIS HANDBOOK

FIGURE 5.21: HDT ANSWER LISTING

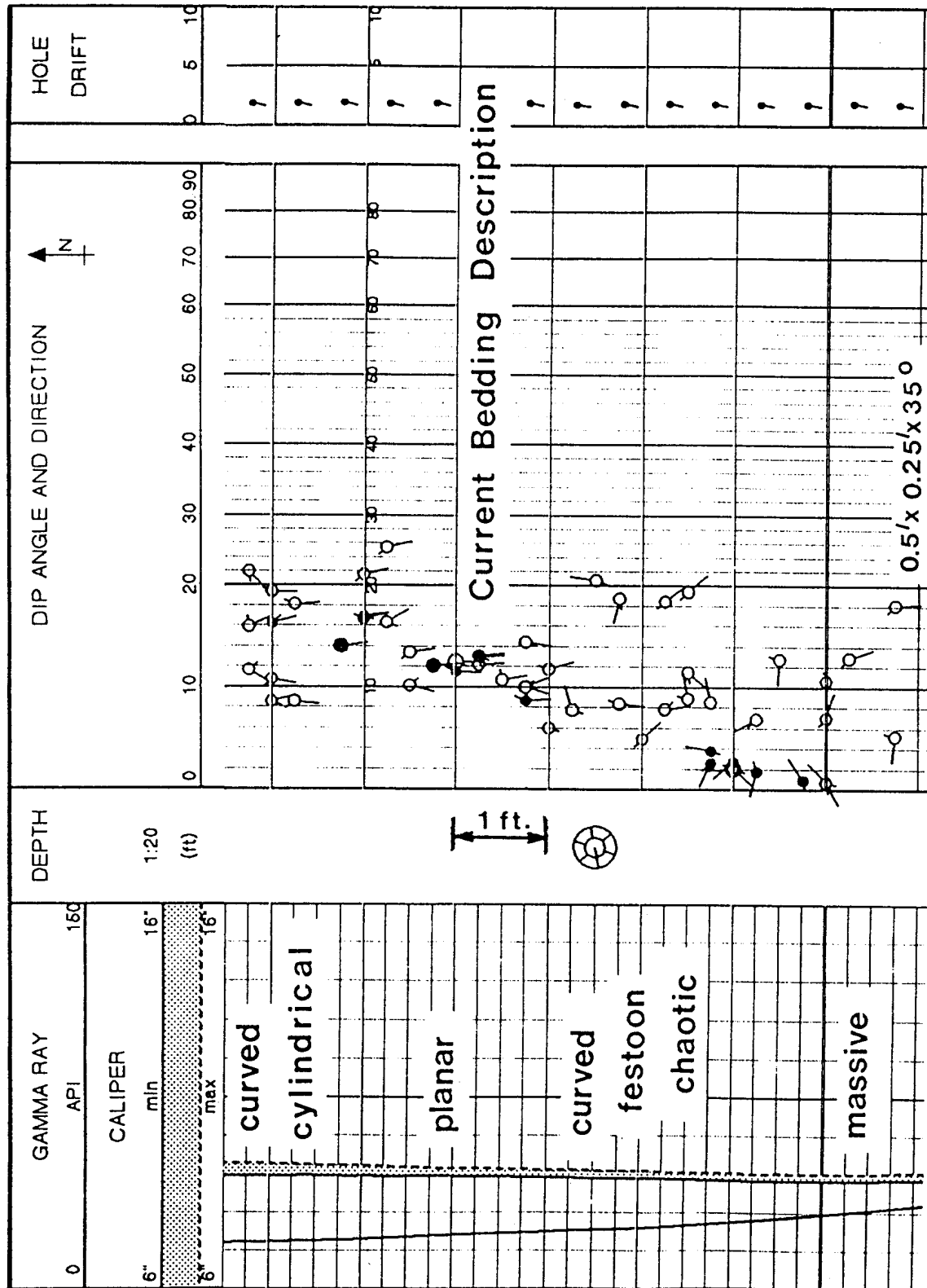
1	2	3	4	5	6	7	8	9	10	11	12
*****	*****	*****	*****	*****	*****	*****	*****	*****	*****	*****	*****
* DEPTH	DIP	DIP	DEV	DEV	DIAM	DIAM	LB	Q	PLA	CLB	MAX
*		AZM		AZM	1-3	2-4	GI				
*****	*****	*****	*****	*****	*****	*****	*****	*****	*****	*****	*****
* 5896	3.0	205	1.9	246	8.7	9.8		B	0	100	50
* 5894	2.1	202	2.0	245	8.6	9.9		A	45	100	54
* 5892	3.2	195	2.0	243	8.5	10.0		A	100	100	59
* 5890	3.1	206	2.0	243	8.6	9.8		A	0	100	57
* 5888	2.6	230	2.0	243	8.6	9.9		A	0	100	57
* 2 5886	3.4	230	2.1	243	8.7	10.1	**	A	44	100	53
* 5884	2.4	215	2.1	243	8.8	10.0		A	100	100	74
* 5882	2.6	187	2.1	243	8.8	9.8		*	0	43	76
* 5880	5.2	259	2.0	245	9.0	9.7		C	0	100	35
* 5878	38.2	221	2.0	244	8.9	9.6	**	D	100	100	71
* 5876	4.0	235	2.0	244	8.8	9.8	**	C	100	100	86
* 3 5874	3.5	236	2.0	245	8.7	10.0	**	B	100	100	78
* 5872	2.8	228	2.0	245	8.8	10.1	**	C	100	100	73
* 5870	2.1	230	2.0	244	8.7	10.1	**	C	40	100	85
* 5866	5.2	228	2.2	245	8.8	10.6		B	0	100	91
* 1 5864	NO CORR		2.1	244	9.0	10.6					
* 5862	24.4	140	2.1	245	9.1	10.6		*	0	0	35
* 4 5860	30.7	24	2.1	244	8.8	10.6		*	0	0	6
* 5858	6.3	234	2.1	244	8.7	10.4		A	0	54	27
* 5856	24.3	319	2.2	245	8.7	10.5		*	0	20	23
* 5854	1.1	222	2.3	244	8.8	10.6		*	0	30	44
* 5852	18.7	306	2.4	243	8.7	10.5		B	0	100	37
* 5850	21.9	303	2.3	244	8.5	10.5		D	0	100	50
* 5848	1.8	114	2.3	244	8.5	10.5		B	0	100	73
* 5846	1.4	223	2.2	244	8.5	10.5	**	B	17	57	84
* 5844	2.1	196	2.1	244	8.4	10.5	**	A	100	100	73
* 5842	2.6	211	2.2	243	8.3	10.6	**	A	100	100	68
* 5840	3.9	232	2.3	243	8.3	10.6	**	C	100	68	58
* 5838	1.7	219	2.3	244	8.5	10.6		*	0	33	72
* 5836	3.6	132	2.2	245	8.5	10.7	**	C	10	100	61
* 5832	1.4	218	2.3	243	8.5	10.8	**	A	100	100	84
* 5830	1.6	221	2.3	243	8.4	10.9	**	A	100	100	82
* 5828	1.5	201	2.4	243	8.4	10.9	**	B	100	100	72
* 5826	1.7	107	2.4	244	8.4	10.9	**	B	11	100	84
* 5824	.7	193	2.4	244	8.3	10.9		C	0	100	90
* 5822	1.5	206	2.4	243	8.2	10.8		C	0	100	85
* 5820	2.5	260	2.4	242	8.2	11.0		*	0	10	42
* 5818	1.7	196	2.4	240	8.2	11.2	**	D	100	100	86
* 5816	.4	230	2.4	240	8.4	11.3	**	D	10	100	82
* 5814	1.3	189	2.4	238	8.4	11.4	**	A	33	100	59
*****	*****	*****	*****	*****	*****	*****	*****	*****	*****	*****	*****

1. Computation attempted unsuccessfully.
2. **Four-pad logic.
3. "Best-Fit" dip determination, good planarity.
4. *Quality not rated (coherence factor not computed).

Illustration courtesy of Schlumberger

THE LOG ANALYSIS HANDBOOK

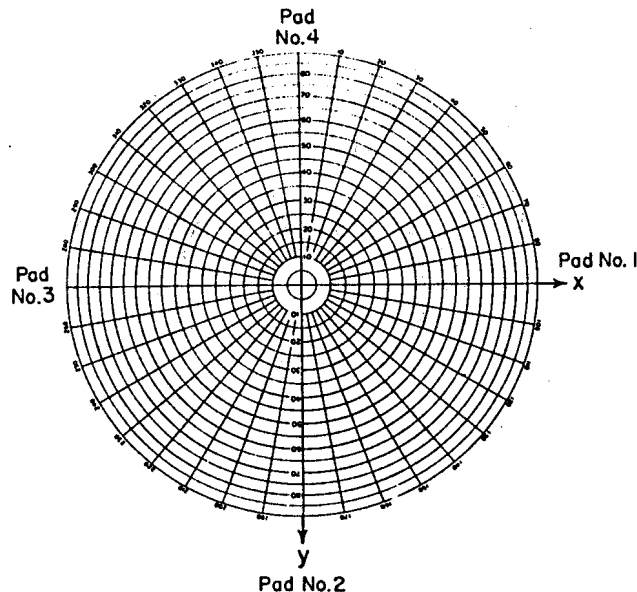
FIGURE 5.22: SIX ARM DIPMETER ANSWER PLOT



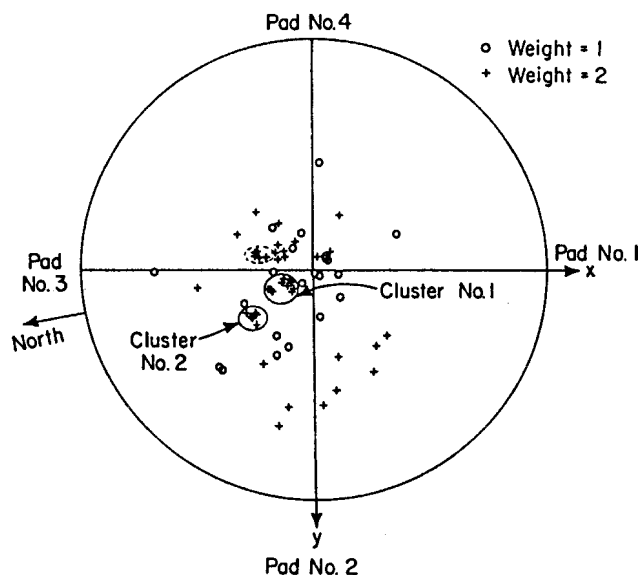
From: The Six Arm Dipmeter, J.F. Goetz, Trans CMLS, 1985

THE LOG ANALYSIS HANDBOOK

FIGURE 5.23: DIP CLUSTERING TECHNIQUE



- Two-dimensional map representing hemisphere scaled in circles of dip angle (θ) and radii of azimuth (ϕ).



ADJACENT-CURVE DISPLACEMENTS

DEPTH (FEET)	H12	H23	H34	H41	PAZ (DEGR)
OPEN ZONE					
3858	3.71	-0.69	3.43	-3.27	181
3856	0.81	-0.65	-0.90	0.78	192
3854	0.97	-0.43	-1.24	-0.70	189
3852	0.92	-0.46	-1.39		182
3850	0.77	-0.20	-1.45	0.59	178
3848	0.70	-0.12	-4.46		176
3846		-0.31	-4.82		180
STABLE ZONE					
3844	0.32	-0.58	-0.37	0.45	195
3842	0.11	-0.79	-0.34	0.36	205
3840	-0.04	-0.93		0.65	208
3838	-0.25	-1.03	0.44	0.73	205
3836	-0.34	-0.99	0.39	0.79	202
OPEN ZONE					
3834	-0.29	4.20	-0.29	1.26	203
3832	3.58	1.46			203
3830	-2.97	1.42	-0.06	1.07	202
3828	-3.24		1.77	0.74	200
3826	-3.21	-0.40	1.21	0.49	201
3824	-0.90	-0.28	1.10	0.37	204
3822	-1.04	-0.04	1.12	0.51	202
3820	-4.45	5.10	1.21	3.22	196
3818	0.63	0.11	6.88	-0.07	191
3816	0.70	0.04			191
OPEN ZONE					
3814	-0.90	1.04	-0.80		188
3812	-0.57	0.97			185
3810	0.16	0.99	0.87	-1.92	182
3808			0.79	-1.16	177
3806	-2.42	1.56	1.27	-0.11	172
3804		0.19	-4.47		171
3802					174
3800	-5.80	-6.00	0.38	-9.13	183
3798		5.49	0.93	-2.31	192
3796	0.81	0.11	-0.78		194

From: CLUSTER: A Method for Selecting Most Probable Dip,
Hepp & Dumestre, SPE 5543, 1975

THE LOG ANALYSIS HANDBOOK

FIGURE 5.24: CLUSTER INPUT LISTING

DEPTH (FEET)	CALIPERS		CURVE DISPLACEMENTS						MAX	WELL DEVIATION		TOOL ORIENTATION	
	D13 (INCHES)	D24 (INCHES)	H12	H23	H34 (INCHES)	H41	H13	H24		DEV (DEGREES)	DVAZ (DEGREES)	PAZ (DEGREES)	RB (DEGREES)
3836	8.9	8.4	-0.34	-0.99	0.39	0.79	*	*	57	2.3	7	202	195
3834	8.8	8.4	-0.29	4.20	-0.29	1.26	-1.91		46	2.4	7	203	196
3832	8.8	8.4	3.58	1.46			-0.45		10	2.4	5	203	198
3830	8.8	8.4	-2.97	1.42	-0.06	1.07	-2.22		24	2.4	3	202	199
3828	8.8	8.4	-3.24		1.77	0.74	1.52		31	2.5	2	200	198
3826	8.7	8.4	-3.21	-0.40	1.21	0.49	-3.35		36	2.5	3	201	198
3824	8.6	8.4	-0.90	-0.28	1.10	0.37		0.73	38	2.5	4	204	200
3822	8.5	8.4	-1.04	-0.04	1.12	0.51		0.94	35	2.6	4	202	198
3820	8.6	8.2	-4.45	5.10	1.21	3.22	-3.20		40	2.7	3	196	193
3818	8.5	8.1	0.63	0.11	6.88	-0.07		-0.20	22	2.6	3	191	188
3816	8.5	8.4	0.70	0.04			0.60		27	2.5	5	191	185
3814	8.6	8.5	-0.90	1.04	-0.80		0.11		30	2.4	4	188	183
3812	8.6	8.4	-0.57	0.97			0.62		25	2.3	360	185	184
3810	8.5	8.3	0.16	0.99	0.87	-1.92	*	*	23	2.2	359	182	183
3808	8.5	8.2			0.79	-1.16	-0.17		24	2.1	360	177	177
3806	8.6	8.2	-2.42	1.56	1.27	-0.11			37	2.1	359	172	173
3804	8.6	8.3		0.19	-4.47			-4.16	14	2.1	358	171	172
3802	8.6	8.5		NO CORRELATION						2.0	1	174	172
3802	8.6	8.5		NO CORRELATION						2.0	1	174	172
3800	8.4	8.6	-5.80	-6.00	0.38	-9.13			35	2.0	360	183	182
3798	8.0	8.3		5.49	0.93	-2.31			37	2.0	359	192	192
3796	8.2	8.2	0.81	0.11	-0.78		1.16		14	2.0	2	194	192

From: CLUSTER: A Method for Selecting Most Probable Dip,
Hepp & Dumestre, SPE 5543, 1975

THE LOG ANALYSIS HANDBOOK

FIGURE 5.25: CLUSTER OUTPUT LISTING

DEPTH	DIP	DIP AZM	DEV	DEV AZM	D13	D24	LO GIC	QRC	CE	PAR	MAX	SPD COR
3896	6.4	222	2.1	1	8.5	8.9		C	10	1	38	
3894	8.8	158	2.1	2	8.5	8.9		C	10	1	18	
3892	8.5	190	2.1	4	8.5	9.0		C	10	2	27	
3890	11.4	224	2.1	3	8.5	9.0		A	10	4	33	
3888	5.1	181	2.2	3	8.5	9.0		A	10	7	29	
3886	3.9	200	2.1	4	8.5	9.0		A	10	8	56	
3884	7.7	206	2.1	2	8.5	9.1	**	A	10	8	31	
3882	7.1	196	2.2	0	8.5	9.3		A	10	8	53	
3880	7.6	164	2.2	2	8.5	9.4		A	10	8	51	
3876	18.6	143	2.4	5	8.5	9.2		D	10	1	22	
3874	14.9	146	2.4	4	8.5	9.1	**	B	10	8	8	
3872	13.5	151	2.3	3	8.5	9.1		B	10	5	26	
3870	13.8	152	2.3	1	8.5	9.1		B	10	4	31	
3868	29.7	297	2.4	1	8.5	8.9		D	20	2	30	
3866	12.8	153	2.4	1	8.5	8.8		B	10	5	25	
3864	15.0	165	2.4	1	8.3	8.8		D	10	1	38	*
3862	11.3	177	2.4	1	8.2	8.7		D	10	1	31	*
3856	10.2	119	2.1	9	8.5	8.4	**	A	10	8	40	
3854	10.3	139	2.0	12	8.5	8.4		A	10	5	17	
3852	10.6	129	2.0	14	8.5	8.4		A	10	5	18	
3850	10.1	122	2.0	16	8.5	8.5		A	10	8	35	
3848	6.5	135	2.0	17	8.5	8.5		C	10	3	23	
3844	7.7	112	2.0	16	8.5	8.4		A	10	8	56	
3842	6.1	115	2.1	14	8.5	8.4		A	10	8	49	
3840	6.0	85	2.2	11	8.6	8.4		A	10	5	35	*
3838	6.4	62	2.3	7	8.8	8.4	**	A	10	8	49	
3836	6.4	59	2.3	7	8.9	8.4	**	A	10	8	57	
3830	10.7	24	2.4	3	8.8	8.4		D	10	1	24	
3828	23.8	346	2.5	2	8.8	8.4		D	20	1	31	
3826	8.4	354	2.5	3	8.7	8.4		D	10	2	36	
3824	6.6	353	2.5	4	8.6	8.4		B	10	8	38	
3822	7.3	345	2.6	4	8.5	8.4		B	10	8	35	
3814	12.0	262	2.4	4	8.6	8.5		D	10	3	30	
3812	10.8	243	2.3	360	8.6	8.4		D	10	3	25	
3810	11.8	258	2.2	359	8.5	8.3	**	D	10	2	23	
3808	12.5	257	2.1	360	8.5	8.2		D	10	3	24	
3806	18.1	250	2.1	359	8.6	8.2		D	10	1	37	
3790	4.6	244	2.0	360	8.5	8.5	**	A	10	8	36	
3788	5.2	257	2.0	0	8.5	8.5		A	10	5	42	
3782	0.5	346	2.0	0	8.3	8.4		A	10	5	26	

From: CLUSTER: A Method for Selecting Most Probable Dip,
Hepp & Dumestre, SPE 5543, 1975

THE LOG ANALYSIS HANDBOOK

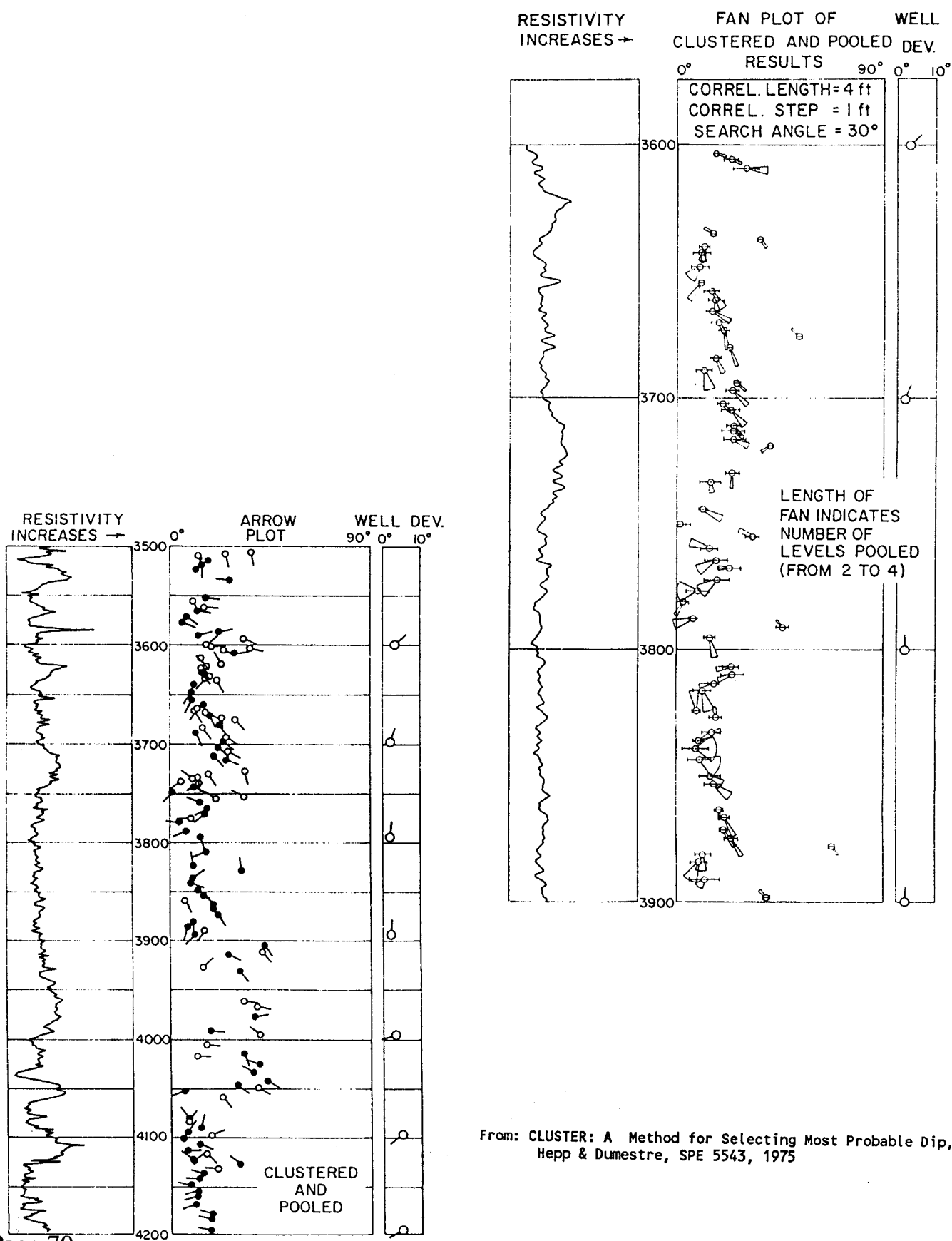
FIGURE 5.26: POOLING OUTPUT LISTING

DEPTH	DIP	AZM	DEV	DVAZ	D13	D24	MAX	NVUS	LP	ANGD	QRP
3850	9.9	124	2.4	16	8.5	8.5	32	21	3	3.3	A
3848	6.7	138	2.4	17	8.5	8.5	23	3	1	0.7	B
3843	6.8	114	2.4	15	8.5	8.4	46	29	4	3.6	A
3839	5.5	87	2.7	10	8.7	8.4	44	25	4	4.0	A
3836	6.3	65	2.7	7	8.9	8.4	56	24	3	1.2	A
3832	10.4	83	2.8	5	8.8	8.4	29	4	2	2.7	C
3830	8.5	89	2.8	3	8.8	8.4	24	1	1	57.3	D
3827	11.7	352	2.9	3	8.8	8.4	27	6	2	1.8	A
3824	6.0	354	2.9	3	8.7	8.4	44	26	4	1.3	A
3822	7.0	343	3.0	4	8.5	8.4	35	8	1	2.1	B
3816	7.6	160	2.9	4	8.5	8.3	25	13	4	2.6	C
3813	11.1	257	2.8	2	8.6	8.4	26	7	3	1.6	C
3810	16.7	244	2.6	360	8.5	8.3	31	11	3	3.5	C
3807	16.2	254	2.5	360	8.5	8.2	28	5	3	2.4	C
3803	19.1	235	2.4	359	8.7	8.4	9	1	1	57.3	D
3795	9.8	164	2.4	1	8.3	8.3	34	10	4	1.6	C
3793	6.7	158	2.4	0	8.5	8.5	43	2	1	1.7	D
3791	36.6	320	2.4	360	8.5	8.5	29	4	2	2.9	C
3788	4.8	249	2.4	1	8.5	8.5	33	18	4	1.3	A
3781	1.5	240	2.4	360	8.4	8.4	28	13	3	1.9	C
3777	6.1	267	2.4	2	8.5	8.5	33	26	4	3.4	A
3775	8.9	272	2.4	4	8.5	8.5	39	5	1	2.3	B
3772	11.8	233	2.4	3	8.5	8.5	53	29	4	4.0	A
3770	12.5	233	2.4	2	8.5	8.5	47	8	1	4.6	B
3768	15.6	264	2.4	3	8.5	8.5	71	14	2	3.7	A
3765	11.7	239	2.4	3	8.5	8.6	60	32	4	3.5	A
3760	9.4	288	2.4	3	8.5	8.7	27	20	4	2.4	A
3758	10.1	291	2.4	3	8.5	8.6	42	8	1	2.0	B
3757	27.9	300	2.4	3	8.5	8.5	70	1	1	57.3	D
3755	23.6	296	2.4	3	8.5	8.3	72	19	3	3.0	C
3753	23.1	305	2.4	4	8.5	8.2	63	2	1	2.7	D
3750	0.7	88	2.4	7	8.5	8.5	28	21	4	3.3	C

From: CLUSTER: A Method for Selecting Most Probable Dip,
Hepp & Dumestre, SPE 5543, 1975

THE LOG ANALYSIS HANDBOOK

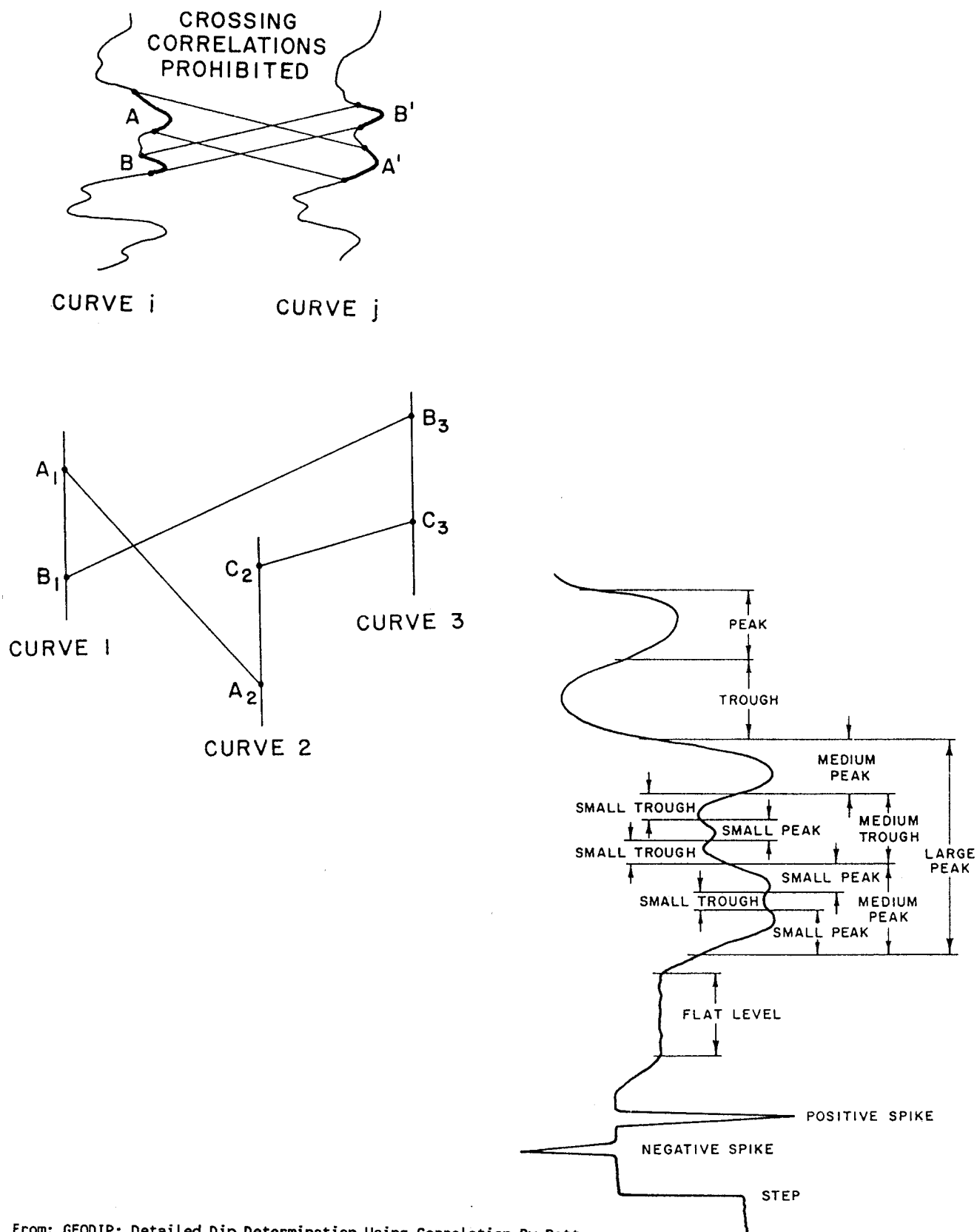
FIGURE 5.27: POOLED AND FAN PLOTS



From: CLUSTER: A Method for Selecting Most Probable Dip,
Hepp & Dumestre, SPE 5543, 1975

THE LOG ANALYSIS HANDBOOK

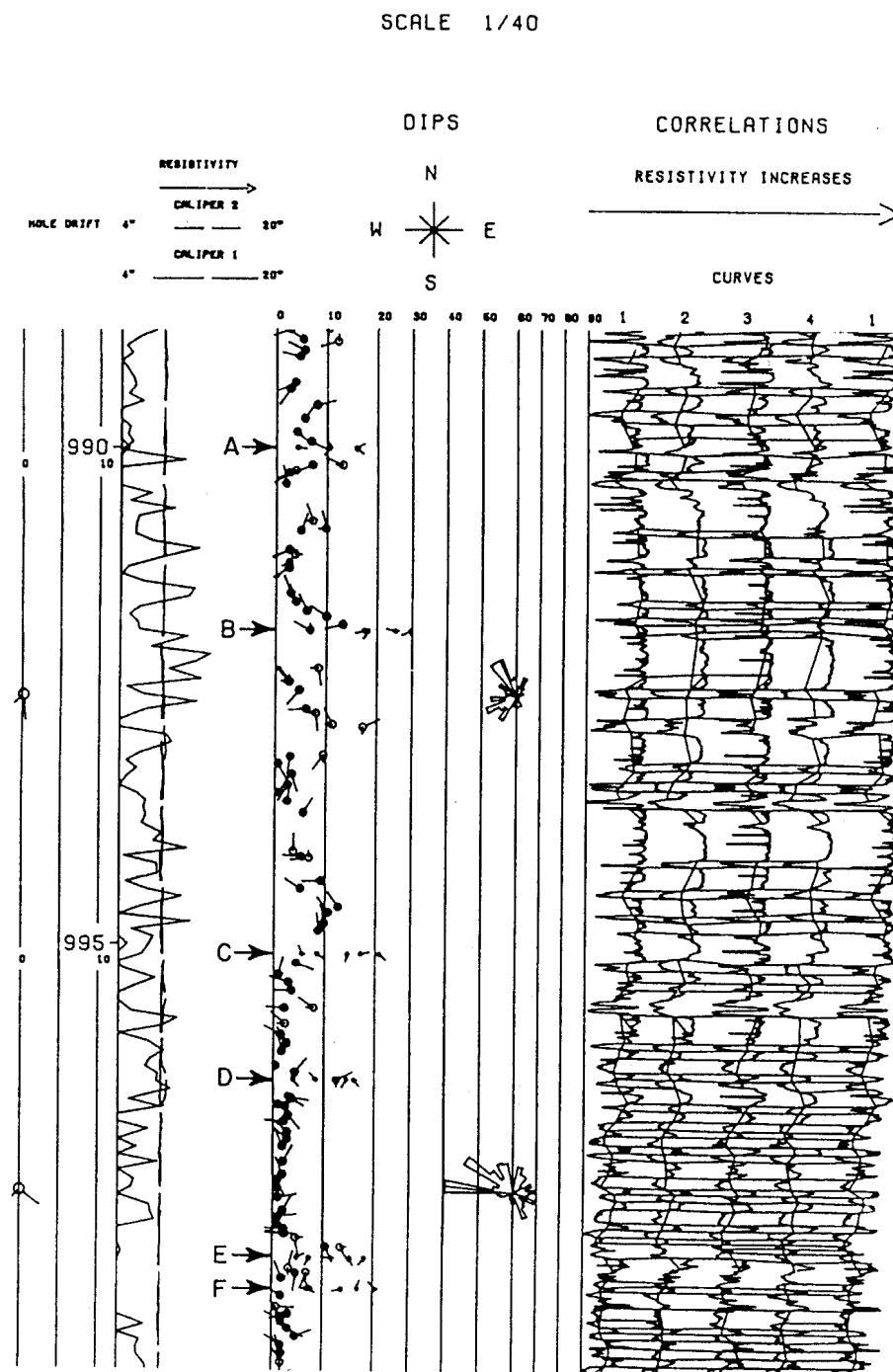
FIGURE 5.28: PATTERN RECOGNITION RULES



From: GEODIP: Detailed Dip Determination Using Correlation By Pattern Recognition, P. Vincent et al, SPE 6823, 1977

THE LOG ANALYSIS HANDBOOK

FIGURE 5.29: GEODIP ANSWER PLOT



From: GEODIP: Detailed Dip Determination Using Correlation By Pattern
Recognition, P. Vincent et al, SPE 6823, 1977

THE LOG ANALYSIS HANDBOOK

FIGURE 5.30: GEODIP OUTPUT LISTING

```

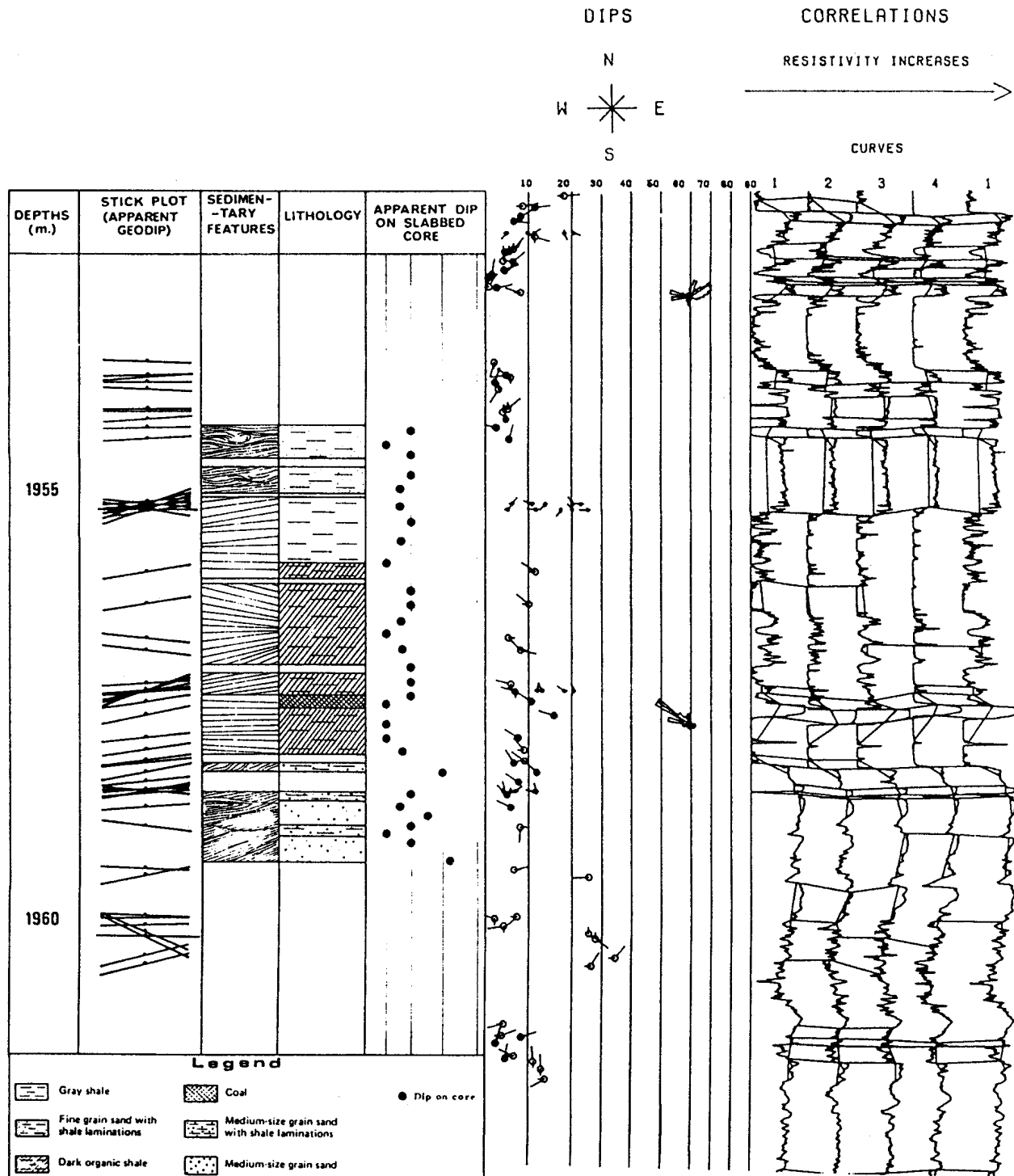
*****
* DEPTH      DIP AZI PLA  DEV  AZDEV 1/2  CORRELATED SAMPLE AND TYPE OF ELEMENT *
* (ft)
*
* CURVE 1    CURVE 2    CURVE 3    CURVE 4
*****
* 10363.33   14.6 144    0    2.8 239    2    8521 4    8527 4    0 0    8529 2 *
* 10363.77   14.1 161    0    2.6 237    1    8497 4    8500 4    0 0    8507 2 *
* 10363.82   13.9 162    0    2.6 237    2    8497 3    0 0    8510 1    8507 1 *
* 10364.35   13.2 170    0    2.8 241    1    8468 3    0 0    8479 1    8478 1 *
* 10364.35   12.9 170    0    2.8 241    1    0 0    8469 5    8479 5    8478 5 *
* 10372.05   13.4 61     0    2.8 235    2    8000 3    8007 3    0 0    8002 3 *
* 10372.73   9.2 5       0    2.8 239    1    7960 3    7963 3    0 0    7955 3 *
* 10372.73   9.2 5       0    2.8 239    2    7960 4    7963 4    0 0    7955 4 *
* 10373.10   9.2 39      0    2.4 241    1    7935 4    7940 4    0 0    7934 4 *
* 10373.17   6.9 6       88   2.4 241    2    7935 3    7940 3    7934 1    7934 3 *
* 10373.38   4.5 88      93   2.4 241    1    7921 3    7923 3    7923 1    7924 3 *
* 10373.38   4.5 88      93   2.4 241    2    7921 4    7923 4    7923 2    7924 4 *
* 10374.02   3.0 100     95   2.8 233    1    7886 4    7886 4    7886 2    7888 4 *
* 10374.02   3.0 100     95   2.8 233    2    7886 3    7886 3    7886 3    7888 3 *
* 10374.33   4.0 48      99   2.6 230    1    7866 3    7867 3    7867 3    7866 3 *
* 10376.02   4.1 295     0    2.8 228    2    7764 3    0 0    7758 3    7760 1 *
* 10376.30   1.4 286     0    2.8 228    1    7751 3    0 0    7747 3    7749 1 *
* 10376.37   4.1 182     88   2.8 228    2    7751 4    7744 2    7747 4    7749 4 *
* 10376.57   2.4 319     90   2.8 232    1    7738 4    7734 2    7734 4    7733 4 *
* 10376.57   6.9 340     0    2.8 232    2    7738 3    0 0    7734 3    7733 3 *
* 10376.77   2.7 114     0    2.4 235    1    7721 3    0 0    7721 3    7722 3 *
* 10377.97   6.2 340     0    2.8 223    2    0 0    7650 3    7646 5    7645 3 *
* 10378.42   8.4 49      0    2.8 226    1    0 0    7621 3    7622 5    7618 3 *
* 10385.40   13.0 326     92   2.8 226    2    7210 4    7211 4    7204 4    7199 4 *
* 10385.73   7.1 306     92   2.6 228    1    7190 4    7187 4    7183 4    7182 4 *
* 10385.98   5.7 305     88   2.8 223    2    7170 2    7171 4    7164 2    7167 2 *
* 10386.17   5.7 275     96   2.8 223    1    7162 2    7158 4    7154 2    7156 2 *
* 10397.12   3.3 92      0    2.6 219    2    6490 3    6488 1    0 0    6490 3 *
* 10397.42   2.2 103     0    2.8 217    1    6471 3    6469 1    0 0    6470 3 *
* 10398.78   6.0 116     0    2.8 223    2    0 0    6387 4    6387 4    6391 4 *
* 10399.07   7.8 94      0    2.8 219    1    0 0    6368 4    6370 4    6374 4 *
* 4 DIP COMPUTATIONS. TR1 37 305 TR2 45 273 TR3 35 244 TP4 15 271
* 10400.05   32.5 272    54   2.6 221    2    6318 4    6325 4    6315 4    6286 2 *
* 4 DIP COMPUTATIONS. TR1 39 308 TR2 45 279 TR3 33 254 TP4 18 292
* 10400.33   33.7 283    59   2.8 221    1    6296 4    6308 4    6300 4    6268 2 *
*****

```

From: GEODIP: Detailed Dip Determination Using Correlation By Pattern Recognition, P. Vincent et al, SPE 6823, 1977

THE LOG ANALYSIS HANDBOOK

FIGURE 5.31: GEODIP COMPARED TO CORE



From: GEODIP: Detailed Dip Determination Using Correlation By Pattern Recognition, P. Vincent et al, SPE 6823, 1977